Relationship of firing intervals of human motor units to the trajectory of post-spike after-hyperpolarization and synaptic noise

Peter B. C. Matthews

University Laboratory of Physiology, Parks Road, Oxford OX1 3PT, UK

1. Interspike interval distributions from human motor units of a variety of muscles were analysed to assess the role of synaptic noise in excitation. The time course of the underlying post-spike after-hyperpolarization (AHP) was deduced by applying a specially developed transform to the interval data. Different firing rates were studied both by varying the firing voluntarily, and by selecting subpopulations of spikes for a given firing rate from long recordings with slight variations in frequency.

2. At low firing rates the interval histograms had an exponential tail. Thus at long intervals, the motoneurone was randomly excited by noise and its post-spike AHP was complete. This contrasts with the firing produced by intracellular current injection in the cat, when the membrane potential increases linearly until threshold is reached. The interval histogram was therefore analysed with the aid of a model of synaptic excitation to deduce the mean 'trajectory' of membrane voltage in the last part of the interspike interval.

3. The computer model, described in the Appendix, was used to determine the effect of the mean level of membrane potential on the probability of a spike being excited, per unit time, during an on-going interspike interval. All variables were treated as voltages, with synaptic noise simulated by time-smoothed Gaussian noise. This enabled an interval distribution to be transformed into a segment of the underlying trajectory of the membrane potential; the potential was expressed in terms of the noise amplitude and the spike threshold.

4. At low firing rates, the equilibrium value of the membrane voltage trajectory lay well below threshold; the deviation typically corresponded to the standard deviation of the noise or more. The noise standard deviation was estimated to be about 2 mV.

5. With increasing mean firing rate, the near-threshold portion of the trajectory obtainable from the histogram occurred earlier, was steeper and rose to a higher level. Trajectories for different firing rates fell on the same curve after shifting them vertically by varying amounts. The curve was taken to represent the AHP of the motoneurone and was closely exponential. The shift of the trajectory gave its mean synaptic drive. The duration of the AHP varied between units and was longer than average for units from soleus muscle.

6. Further modelling showed that summation of noise with the AHP can explain the well-known changes in discharge variability that occur as firing rate increases.

7. It is concluded that synaptic noise plays a major role in the excitation of tonically firing human motoneurones and that the noiseless motoneurone with a linear trajectory provides an inadequate model for the conscious human. This is of interest in relation to various standard measures of human motor unit activity such as short-term synchronization.

In their pioneer recordings in 1929, Adrian & Bronk found that during a maintained voluntary contraction, human motor units fire at a slow regular rhythm. With the advent of digital computers, the determination of interspike interval histograms for such discharges has become routine. These histograms commonly approximate to a Gaussian distribution with a coefficient of variation of 10–25%, as has long been recognized (Tokizane & Shimazu, 1964; Clamman, 1969). The variability of the discharge is greater for low firing rates, with the coefficient of variation of the interval distribution tending to increase with the mean. Detailed analyses have regularly shown departures from

normality, with a definite pattern emerging. Kranz & Baumgartner (1974) noted that their 'interval histograms were narrow and symmetrical at fast rates, broader and skewed to the right at slower rates'; this was also found by Person & Kudina (1972). Enoka, Robinson & Kossev (1989) recently gave formal description to such behaviour and stated that 'none of the distributions were Gaussian ($P < 0{\cdot}001$) because of a greater degree of kurtosis and a skew towards longer intervals (positive skew)'. The Weibull distribution will fit a range of such non-Gaussian histograms (De Luca & Forrest, 1973), but its various parameters bear no relation to physiological variables. Recently, the effects of synaptic noise have been studied with a random walk model with infinite memory (Warren, Miles & Türker, 1993).

Analysis of the detailed form of the interval distribution is no mere statistical exercise, since it has long been commonplace that study of the detailed timing of spike events can shed light on the mechanisms of spike production, as has been well stated by Moore, Perkel & Segundo (1966). The thesis of the present paper is that, with proper handling, the simple interval histogram of the motor unit can indeed tell one much about the factors controlling the firing of the motoneurone in the unanaesthetized state in man; the motoneurone is then activated physiologically by the tonic interplay of synaptic excitation and inhibition, with resultant synaptic membrane noise. In the cat, Calvin & Stevens (1968) showed that synaptic noise was responsible for slight deviations from normality of interval histograms obtained from motoneurones during the intracellular injection of current. Large departures from normality have been seen in neurological disease (Freund, Dietz, Wita & Kapp, 1973), giving further impetus to studying the underlying factors.

The pattern of firing *per se* has also long been of interest in relation to the noisiness of signal transfer. More recently, synaptic noise has been recognized as having a crucial effect on various experimental measures of synaptic action such as the relation between the form of a brief excitatory input, or EPSP, and the consequential change in motoneuronal firing in a post-stimulus time histogram (Kirkwood, 1979; Gustafsson & McCrea, 1984; Midroni & Ashby, 1989). Likewise, noise affects the extent to which the discharges of a pair of motor units may be synchronized when both are activated by branches of the same presynaptic axon (Kirkwood & Sears, 1991; Nordstrom, Fuglevand & Enoka, 1992).

The present experiments arose from an incidental observation made during an earlier single motor unit study (Matthews, 1994), namely that the falling phase of histograms with a tail of long intervals (positive skew) may be approximately exponential, a feature of well-known importance (Moore *et al.* 1966). Surprisingly, such behaviour does not seem to have attracted previous attention for the motor unit although it immediately suggests that the human motoneurone is then being randomly excited by synaptic noise, following the completion of the membrane after-hyperpolarization (AHP) left by the preceding spike. In other words, the total duration of the AHP 'trajectory' may be shorter than many interspike intervals, making the pattern of excitation in conscious man quite unlike that seen with intracellular current injection in the anaesthetized cat, when the potential increases linearly up to threshold and a spike is initiated (Schwindt & Calvin, 1972). It then becomes of considerable interest to determine how far the final equilibrium membrane potential lies below threshold during physiological activation of the motoneurone in man. A simplified model of excitation, described in the Appendix, was therefore used to determine the probability of firing in terms of the membrane potential and the amount of synaptic noise. This showed that for low firing frequencies, the equilibrium membrane potential was subthreshold by an amount about equal to the standard deviation of the noise.

The model was also used to deduce the voltage trajectory of the AHP (expressed in units of the noise variance) over the whole period covered by the interval histogram. Only the last part of the AHP could be charted, but the amount covered was extended by studying a number of firing frequencies. AHPs from different motoneurones were found to differ in their time course, as is well known for directly recorded AHPs; in addition, their apparent size might vary between motoneurones, suggesting differences in the noise level. The AHPs proved to be approximately exponential over the range studied, in line with the time course of the underlying conductance change. Reversing the causal chain, synthetic interval histograms were produced by combining an exponential AHP with the noise in the model motoneurone; the variance of the histograms decreased appropriately as the firing rate increased.

The special feature of the modelling was the deduction of two inversely related transforms relating probability of firing to membrane potential and vice versa, in the presence of appreciable synaptic noise. These enabled an interval histogram to be predicted from a trajectory and, more especially, a trajectory to be estimated from a histogram. The chief uncertainty arose from ignorance of the membrane time constant of the particular neurone studied; this value was used to smooth the Gaussian noise that simulated the synaptic noise and affected the precise transform obtained. In addition, inaccuracy was probably introduced by using a highly simplified model motoneurone, and the matter merits further study with more detailed modelling. Attention was concentrated on the low-frequency noise-induced firing that occurred when the mean value of the membrane potential was below threshold. Previous modelling of the motoneurone has been largely concerned with the higher-frequency firing induced by steady currents that bring the membrane to threshold, when noise is relatively unimportant (Kernell, 1968; Baldissera & Gustafsson, 1974*a*, *b*; Ashby & Zilm,

1982). However, synaptic noise has always been at the centre of modelling the physiological activation of respiratory motoneurones during breathing (Kirkwood, 1979; Kirkwood & Sears, 1991). The present findings, whether based on modelling or experiment, may thus be of some general interest by virtue of their concentration on a relatively neglected but essential part of the normal firing range of a neurone.

Two broad conclusions can be drawn from the experiments; they seem secure even if certain details of the modelling should prove seriously simplistic. First, the human interval histogram contains valuable information about the trajectory of the AHP and the level of synaptic noise. Most notably, at low firing rates the mean value of the membrane potential never reaches threshold and firing is entirely due to noise. Second, the variety of shapes of the distributions, with their departures from a Gaussian curve and their variation with firing frequency, can be attributed to an interaction between appreciable on-going synaptic noise and the trajectory of the AHP. The findings affect the interpretation of several indices of synaptic activity, such as those for short-term synchronization between a pair of units.

METHODS

Single motor unit recordings were made in seven neurologically normal subjects aged 20–65 years (5 male, 2 female). All gave informed consent according to the Declaration of Helsinki; the procedures involved no risk of harm. Sixty-three units were studied, forty-three of them from the author, a variety of whose muscles was studied (biceps brachii, brachioradialis, flexor carpi radialis, first dorsal interosseus of the hand, abductor digiti minimi (ADM), soleus, tibialis anterior and peroneus longus); in other subjects, just one or two muscles were examined (biceps, flexor carpi radialis or brachioradialis). A minimum of 2000 spikes was collected for each unit, but normally very much longer discharges were obtained; over 80 000 spikes were recorded from three of the units (of the 63 units, 4 had 2000–3000 spikes, 32 had 3000–10 000 spikes, and 25 had more than 10 000 spikes). The mean firing rate was usually below 10 Hz (range, 5·6–15·6 Hz). The collection of large numbers of spikes from a given unit was done in a series of separate recording periods of 5–30 min duration, in each of which the subject endeavoured to keep the unit firing at a constant low mean rate; subjects were provided with both visual and auditory feedback of the discharge (the visual feedback consisted both of the on-going spike train displayed on a slow time base and the individual spikes on a high-speed sweep; the running mean firing rate was not provided because of its potential to produce oscillatory behaviour). The subject was told to make any corrections to the firing rate rather gently as rapid changes interfered with the analysis (see Fig. 1). Collection ceased when the subject found it difficult to continue to control the unit, or if another unit started to interfere with the recording. The various recordings from a given unit were normally very similar and no systematic differences were found between the beginning and end of an individual collection period when these were analysed separately. The contractions were normally weak and the subject did not become fatigued.

Most units (43/63) were recorded with surface electrodes, as already described (Matthews, 1994). This greatly facilitated the collection of a large number of spikes from a given unit and helped ensure that the same unit was indeed studied throughout; these 'surface' units could thus be analysed in detail and so contributed most of the present data. The two active electrodes (1–3 mm diameter, separation about 1 cm) were placed over the surface of the muscle; a suitable location was determined by trial and error, but the edge of the muscle belly was frequently a favourable site. An earth was placed in the mouth. Surface recording inevitably favours the selection of low-threshold units; however, an appreciable contraction might be present, and a large spike was often recorded in the presence of smaller background spikes. Pre-existing shorter recordings obtained from twenty units with bipolar needle electrodes were thus also included in the analysis as a control; the results were indistinguishable, confirming that the surface recording had not selected an atypical population of units (needles were inserted into the belly of flexor carpi radialis of three subjects, including the much-studied author). In most of these experiments the muscle was being stretched sinusoidally (P. B. C. Matthews and P. Bawa, unpublished study), but trials were chosen for analysis in which this had only a very weak effect on the unit in question; the simple interval distribution is then almost entirely unaffected (Matthews, 1994, especially Figs 8 and 9; cyclic modulation always below 45% and usually much less).

Spike train analysis

The unit recordings were amplified (bandpass, 100 Hz to either 1 or 3 kHz) and then fed to a simple level detector to produce a standard pulse which was supplied to the digital input of a computer for the initial on-line analysis; the unitary spikes were also stored on a separate digital tape-recorder (bandpass, 0–20 kHz) to permit repeat analysis if desired. The triggering of the pulse by the spike was monitored continuously during the experiment to ensure that the same unit was being studied throughout and that it remained truly single. The computer measured the time of occurrence of every spike to within 0·1 ms and constructed a spike interval histogram with a bin width of 5 ms. At the end of each trial both the interval histogram and the serial spike times were stored on disk for further analysis. This was done with a variety of programs, purpose-written in Turbo Pascal; these both computed various conventional statistics and performed various special functions, as detailed below. For these subsequent analyses, individual runs of data with similar firing frequencies were commonly combined.

Calculation of probability. The conventional interval histogram was routinely transformed into a plot of the probability of an on-going interval being terminated during the course of a bin (the interval 'death rate', see Results). As a first approximation, this is given by the number of spikes occurring in a given bin of the interval histogram divided by the sum of the spikes in all bins with the same or greater interval. In other words, this gives the probability, for each time, that the unit will fire in the immediate future, provided that it has not already done so. Such probabilities have already been calculated for certain other neurones (Goldberg, Adrian & Smith, 1964; Moore *et al.* 1966), but there is no agreed name for the resulting probability function.

Even when the underlying continuous probability function remains constant throughout the duration of the bin, the estimate given above will be slightly in error when the bin width is appreciable. This is well known for the analogous situation of radioactive decay, and error is easily avoided by comparing the

number of spikes remaining to be discharged at the beginning and end of each bin. Specifically,

$$P = [\ln(N_0/N_1)] / \text{bin width},$$

where P is the probability of a spike being fired per unit time, averaged over the bin; N_0 and N_1 are the sum of all subsequent bins in the simple interval histogram, with N_0 including the bin whose P is being measured and N_1 excluding it (ln is the natural logarithm). This assumes that the probability of a spike being fired is a continuous process, reducing the population of remaining spikes available to fire throughout the course of a finite bin. The calculations were terminated when the remaining counts had been reduced to a fixed small proportion (typically 2%) of the initial count.

More correctly, P (as given above) is the rate constant of decay, or death rate, of the population of intervals but in the present context it is conceptually easier to think of P as the estimated probability that a spike will occur within the next millisecond and terminate an individual on-going interspike interval (see Fig. 13). This is acceptable for all qualitative considerations, so P has been routinely referred to as 'probability'; but P was always treated as a rate constant in the various calculations. (The true probability per unit time $= 1 - \exp(-P)$, which tends to P as P tends to zero; thus P correctly gives probability when the unit of time is suitably small.) The exponential equation allows the rate constant to be estimated from coarsely binned data in which the measured count falls appreciably from bin to bin.

Cleaning the spike train. Inevitably, occasional false triggers occurred, due to the intrusion of other units. The frequency of their occurrence could be approximately estimated from the interval distribution, since every false trigger splits a normal interval into a pair of false shorter intervals. These displayed themselves as a series of counts preceding the main body of the interval histogram, which invariably had a well-marked beginning. For most units studied, the proportion of false intervals was below 3% (corresponding to approximately 2% false spikes) and they could be largely ignored; values below 0·5% were sometimes achieved and provided a standard for all the major statements in the present paper. Spikes were only rarely missed; the trigger level was set deliberately low to ensure reliability, at the risk of creating false triggers which mattered less. Any appreciable number of missed triggers declared themselves as a delayed hump in the death rate plots and the data were then discarded (or replayed from tape).

For routine analysis the majority of false intervals were removed from the spike train by the following 'cleaning' procedure, which enabled trains with up to, say, 8% false intervals to be studied with reasonable confidence. First, the start of the interval histogram was identified by simple inspection and a safe cut-off point chosen, usually 10 ms earlier. The whole spike train was then scanned and every interval below the cut-off point eliminated (cf. Nordstrom *et al.* 1992). In addition, both the interval before and the interval after each unduly short interval was also eliminated, since one or other of them must also have been false. Minor further algorithms dealt with the situation where two or more short intervals followed in succession. When the interval was below 5 ms (as sometimes happened when a single complex spike elicited two trigger pulses), the short interval was eliminated without any consequential adjustments.

Intervals above 300 ms, as occur when the subject temporarily fails to keep the unit firing steadily, were also eliminated. As the work progressed, however, it became evident that the 300 ms limit was sometimes removing a few genuine long intervals; for the sake of comparability this was allowed to continue, since it had little overall effect. The 300 ms limit was also used in the modelling. All this cleaning of the spike train must have largely removed the artefactual effects of false triggers on the interval distribution and its statistical parameters, but at the cost of slightly distorting the temporal relations within the train.

Slicing the spike train. Given the long periods for which a given single spike was followed, it could not be expected that even a trained subject would be able to keep it firing at precisely the same mean frequency throughout, and statistical analysis confirmed that this was so (see below). There is no ideal way of analysing such non-stationary series, but the following procedures were employed to subdivide the spike train into components with different mean frequency.

In the initial experiments, the train was subdivided into successive groups of twenty-five spikes and the mean frequency for each such group determined; this may be taken as a measure of the on-going level of central 'drive' upon the motoneurone determined for successive periods spanning 2–3 s. The variance of the population of means was then calculated and compared with the variance of the whole population of intervals. The variance of the means proved to be unduly large, thereby confirming that the mean rate of firing (central drive) was indeed changing with time (analysis of variance regularly gave $F > 6$, with the 1% significance level $<1{\cdot}5$). Groups with means falling within a specified range were then summed to give subpopulations with different central drives; these interval distributions differed in the same way (see Results) as those obtained by the following more elaborate slicing procedure, which was subsequently applied to most of the original data.

In the definitive method used for slicing, the running value of the mean frequency of firing was calculated throughout the course of the spike train as illustrated in Fig. 1. The running mean was then used to allocate each spike individually to the appropriate subpopulation. Ten interspike intervals were used to compute the running mean, spanning a period of approximately 1 s; the period used was centred on each interval in turn, but the interval itself was not used for the average (no appreciable difference was produced by including it). In other words, each spike was tagged with a 'mean rate of firing' based on averaging the five interspike intervals just before it with the five intervals just following it, and the values were then stored. Any desired subpopulation or 'slice', for a mean firing rate falling in a specified frequency range, could then be rapidly assembled and the effect of varying levels of central drive on the interval distribution studied (examples are given in the figure legends). The efficacy of this procedure is shown by findings described in Results.

The variability remaining within a slice was almost entirely due to moment-to-moment variation in spike interval, rather than to slow shifts of drive within the limits chosen (typically spanning 1 s). This is qualitatively apparent for records *A–C* in Fig. 1, and was confirmed by finding that the standard deviation (in milliseconds) of a slice population was only very slightly reduced when the difference between each interval and its running mean was used instead of its absolute value. The slicing cannot, however, have entirely achieved its objective of isolating subpopulations with a fixed synaptic drive; some inappropriate intervals must have slipped through. In particular, as illustrated in Fig. 1*D*, the running mean cannot remain an effective indicator of the on-going synaptic drive when this happens to change rapidly; however, slow

changes as in Fig. 1*E* should not matter greatly. Mistakenly introducing a few unduly long intervals into a histogram for a high level of synaptic drive has a potentially serious effect on the shape of the tail of the histogram, since it contains a small total number of impulses (cf. Fig. 5); this was dealt with by ignoring the last 2% of the spikes in any given histogram and paying less attention to the last 5% when compounding individual trajectories to deduce the AHP (see legends of Figs 7 and 8). In test trials the homogeneity of a slice was not appreciably improved (i.e. its variance only slightly reduced) by measuring the variance of the ten intervals used to calculate each individual value of the running mean, and discarding data with more than average variability.

RESULTS

The following pages describe a series of transformations of the interval histograms of tonically firing motoneurones, leading to a deduction of the time course or trajectory of the underlying mean membrane potential and thus of the post-spike after-hyperpolarization (AHP). Twenty-five motor units with over 10000 recorded spikes were studied particularly thoroughly, since large numbers of spikes reduce the inherent variability of the data and improve the curve fitting, thereby increasing the reliability of the conclusions. Qualitatively similar results were obtained with varying degrees of accuracy for all sixty-three units studied; the final trajectories were always approximately exponential, and for low firing rates came to equilibrium with the membrane potential below threshold. A number of units behaved almost identically and the experiments were continued simply to extend the number of muscles and subjects studied. The text has thus concentrated on the behaviour of individual motor units taken from six muscles, together with a summary plot of the estimated AHPs of eleven units that spanned the range observed. As is to be expected, the findings suggest that the various motoneurones studied differed in their noise level and duration of AHP, as well as in their mean firing rate. No attempt has been made to provide a detailed comparison of such discharge characteristics of the entire sample of motoneurones, as this does little to further understanding. The analysis is developed and explained without any intended loss of generality by reference to well-studied typical examples representative of the whole population of units.

The exponential tail of the interval histogram

When a motor unit was firing at the bottom of its frequency range, its interspike interval histogram regularly displayed a prolonged exponential tail. Figure 2 shows three different representations of such tails for two different units with rather different absolute firing frequencies. The subject was doing his best to keep the units firing at a constant rate throughout the recording; any failure to do so can be allowed for (see later) and does not affect the present issue. The left-hand plots are conventional interval histograms with the percentage of spikes in each bin plotted against the spike interval. Their falling phases, from the arrows onwards, are approximately exponential; this is not, however, a striking feature of such histograms, partly

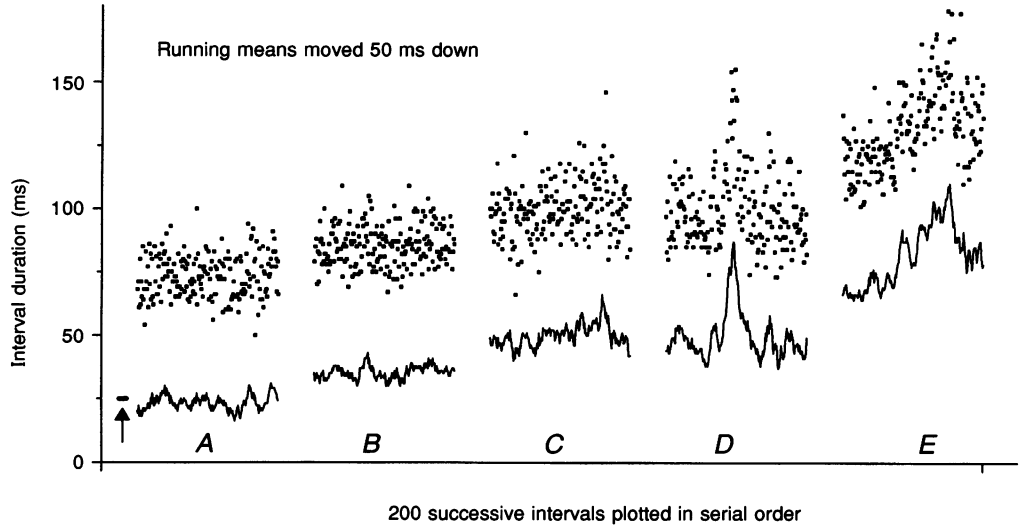

Figure 1. Type of data analysed: serial intervals with running mean for slicing

Top (dots), values of successive interspike intervals plotted in serial order for 5 separate recordings, each lasting approximately 20 s. Bottom (continuous line), their running mean averaged over the duration indicated by the arrow at the left (bar = 10 intervals; plots moved 50 ms down for clarity). *A*, *B* and *C* are from the same unit, when it was firing fairly steadily at 3 different mean rates; the subject was trying to make the unit fire faster in *A*, but *B* and *C* were obtained about 40 s apart in a single recording period. *D* shows a brief slowing of the discharge of the same unit during another recording period; the change was rapid, thus reducing the reliability of the running mean as a measure of the on-going synaptic drive. *E* shows a gradual slowing of another unit, during which the running mean should have remained effective. *A–D*, brachioradialis; *E*, soleus. No intervals removed by cleaning.

because the eye is unduly sensitive to the statistical variation in the size of the vertical steps. With higher firing rates, the interval histogram often approximated to a Gaussian distribution. However, this always provided a poor fit for low firing frequencies. In Fig. 2 the means of the two histograms are appreciably larger than either of their modes (ADM, 111·5 ms *vs.* 90–95 ms; soleus, 171·4 ms *vs.* 155–160 ms) or their medians (103·5 ms and 166·5 ms, for data grouped in 1 ms bins). This shows that both histograms have a positive skew, as was confirmed by measurement of their skew coefficients (1·4 for ADM, 1·1 for soleus).

The centre plots of Fig. 2 show the same data transformed to provide a clearer demonstration that the last part of the histograms was exponential, and pave the way for the analysis of the motoneurone AHP. They are on a semi-log scale and show the percentage of the total number of intervals that were greater than the bin interval in question; each value is plotted as a single point at the end of the bin rather than as a histogram. In this representation the points for the falling phases of the histograms lie on a straight line, indicating an exponential decay. The interpretation of such plots is simplified by considering their familiar application to the statistics of human mortality (cf. Hill, 1961). They give the survival function of a population, showing the percentage of the original cohort that has remained alive to any given age; an exponential decay shows that a constant proportion of the survivors are dying per unit time. In the present case, each member of the population is an interval; one is born after every spike and continues to live until the next spike destroys it. Attention is focused on the interval rather than the spike.

Taking any particular age in a human population, the probability of one of the remaining survivors dying in the next year can be obtained from the slope of the semi-log plots. An equivalent interval death rate was computed point by point for the present data to give the graphs on the right-hand side of Fig. 2 (each point is derived from an adjacent pair of survival values and refers to the mid-point of one of the original bins). The probability of an interval 'dying' within a given period is, of course, the same as that of a spike occurring; the ordinary interval histogram gives the ages at death of the various intervals. The utility of such derivations of the simple interval histogram has long been recognized (Goldberg *et al.* 1964; Moore *et al.* 1966).

After an initial approximately linear increase the death rate plots of Fig. 2 terminated in a constant plateau, with the probability of dying remaining approximately constant over the last part of the distribution. In other words, once a

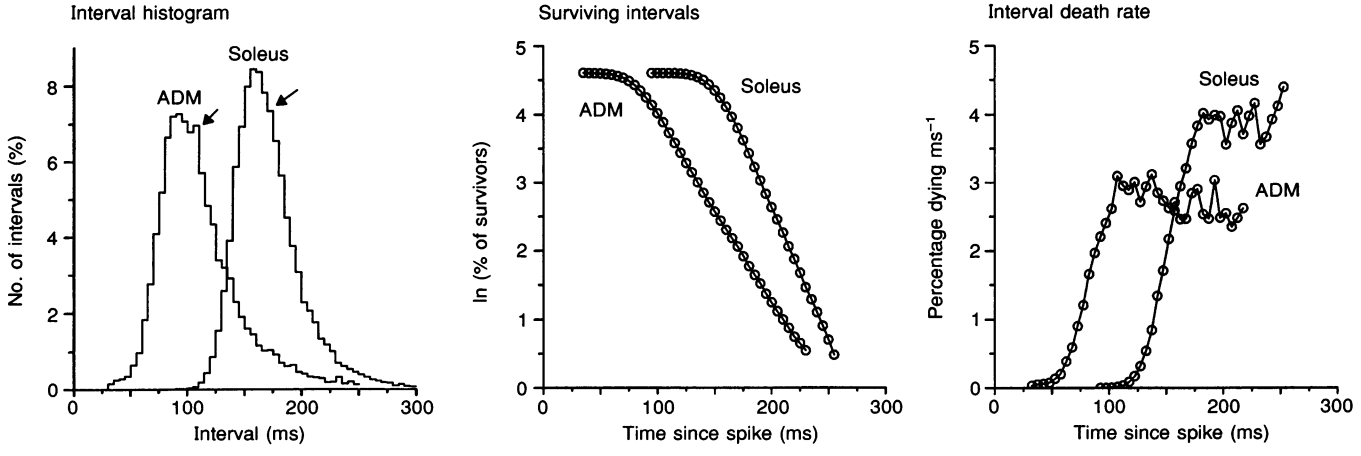

Figure 2. Interval histograms with exponential tails

Three different representations of the distribution of the interspike intervals during slow tonic firing of two different motor units, one in soleus and the other in abductor digiti minimi (ADM). The plots collectively demonstrate that the last part of the distribution is an exponential. Left, conventional interval histogram showing the percentage of intervals falling into a series of 5 ms bins; the arrows mark the start of the exponential decay. Both histograms are positively skewed. Centre, log plot of the number of intervals 'surviving' at the end of each 5 ms bin (i.e. the number of intervals greater than the stated value, expressed as a percentage of the total number of intervals; this was converted to its natural logarithm (ln) with a cut-off at 1–2%). The points for the period of exponential decay lie on a straight line. Right, the death rate of the intervals which have survived up to a given time, expressed as the percentage of the survivors dying per millisecond (i.e. the slope of the survival plot computed for each successive pair of points). The death rate rises to an approximate plateau, corresponding to the exponential tail of the histogram. Both units were firing at the bottom of their frequency range (ADM, 9·0 Hz; soleus, 5·8 Hz) with appreciable interspike variability (coefficients of variation: ADM, 34%; soleus, 17%). 9181 intervals used for ADM and 32101 for soleus after removing 139 stray intervals below 30 ms for ADM (1·4%) and 296 below 90 ms for soleus (0·9%), see Methods; intervals over 300 ms also discarded.

certain critical interval was reached, the probability of a spike being discharged in the next 5 ms stopped increasing and settled at a constant plateau value. Excitation, with the termination of the interval, was then essentially a random process, presumably due to the noise produced in the motoneurone by continuous synaptic bombardment. As a corollary, the motoneurone would appear to have recovered from its previous spike, with its mean depolarization constant. Forty-two per cent of the ADM spikes and 26% of the soleus spikes occurred during the plateau, and so were due solely to noise. The final death rate was slightly lower for ADM than for soleus (3 *vs.* 4% of intervals terminated per millisecond), allowing its plateau to last longer (i.e. until the majority of intervals had died); in other words, the histogram for ADM had a more prolonged exponential tail. However, the chief difference between the two units was in the timing of the ramp phase of increasing death rate; the two slopes were much the same, but the ramp for ADM started over 50 ms earlier, suggesting a considerable difference in the speed of their recovery following a spike.

Reduction of exponential tail with increasing firing rate

On a number of occasions the subject was able to regulate the frequency at which a given unit was firing while maintaining stable recording without undue interference from other units (for 8 units, the mean firing rate was changed by 2 Hz or above, and for another 4 units by 1·4–2 Hz). Figure 3 shows a typical pair of the resulting interval histograms (left), together with their survival and death rate plots. As was usual, increasing the firing rate reduced the duration of the exponential tail. The plateau in the probability plot was raised and shortened but the time at which it began was relatively unaffected; the preceding 'ramp' became steeper with relatively little reduction in its time of onset. Related to all this, the proportion of spikes contributing to the exponential tail decreased as the firing rate increased; in Fig. 3 the proportion fell from 33 to 22%. The interspike variability also decreased, but the histogram remained positively skewed (the coefficient of variation fell from 27 to 19%, with skews of 1·6 and 1·5). The death rate plots in Fig. 3, for the same unit firing at two different rates (8 and 10 Hz), contrast with those of Fig. 2 for two different units with a somewhat similar difference in firing frequency (6 and 9 Hz); varying the firing rate of a unit has a large effect on the final plateau death rate and a small effect on the timing of the ramp of increasing death rate, rather than vice versa as in Fig. 2. Thus the form of the distribution depends upon the properties of the individual motoneurone as well as on the absolute frequency of discharge.

Distributions of subpopulations with different central drive

The data shown so far comprised nearly all of the spikes discharged within a given recording period normally lasting well over 10 min. Many thousands of spikes were collected for each unit to provide a reasonable absolute number of long intervals for measurements on the crucial tail of the histogram, which contains relatively few spikes per bin. The subjects did their best to hold the mean firing rate constant throughout, but were never completely successful (see Fig. 1). Thus the plots in Figs 2 and 3 compound the moment-to-moment variation in the interspike interval, with the effects of any slower changes in the on-going mean firing rate due to variation in the level of central synaptic drive. This limits the accuracy of

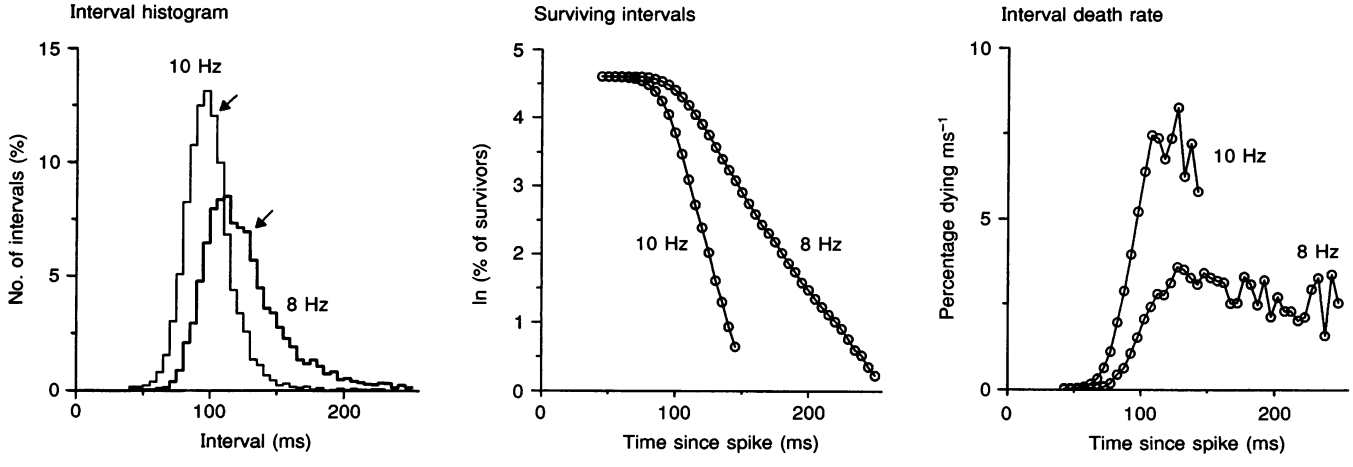

Figure 3. Increasing the firing rate shortens the exponential tail

Comparison of two interval distributions from a motor unit in tibialis anterior when it was being driven to fire at 2 different mean rates (10·1 and 7·9 Hz, values rounded in the figure labels). Same types of plot as in Fig. 2. The exponential decay was faster at the higher frequency and the final interval death rate was greater. The arrows mark the beginning of the exponential decay (5600 intervals used for the higher firing rate and 6547 for the lower one after removing 92 (1·6%) and 33 (0·5%) stray intervals below 40 ms).

the analysis, since in statistical terms the population studied was non-stationary. The situation was improved by slicing the spike train into subpopulations for different ongoing mean frequencies of firing. As described in Methods, this was achieved by calculating the local running value of the mean frequency as it varied with time (mean measured over 10 intervals centred on each interval in turn but not including the interval itself). The local mean firing rate was then used to allocate each spike to a subpopulation of intervals, all of which had occurred when the immediate value of the mean frequency fell within the desired range; this approximately corresponds to selecting spikes discharged at a given level of central drive. Such slicing was not perfect, but it did not create false order out of random variation (see below).

The slicing was partly used to improve the homogeneity of the main interval distribution by removing spikes occurring when the mean central drive happened to be at one or other of its extremes (cf. Fig. 5). More importantly, it was systematically used to select various subpopulations of spikes for different firing rates occurring in the course of a single recording period. This permitted a much fuller study than could be achieved by asking the subject to vary his drive voluntarily. Figure 4 shows an original distribution based on some 30 min of recording (top), together with the results obtained by slicing the spike train into three separate frequency bands (bottom). Increasing firing rate was associated with the interrelated changes seen in Fig. 3 on deliberately varying the central drive. The final death rate increased with the firing rate and the duration of the plateau decreased, while the timing of the ramp leading up to the plateau was relatively unaffected. Such changes were regularly observed on slicing a spike train that might initially have appeared to be homogeneous. In this experiment, the death rate plot of the original recording failed to show a plateau and sagged after an initial peak; likewise the final part of its survival plot is curved, suggesting that it represents the sum of more than one exponential. Such effects inevitably occur on compounding subpopulations with appreciably different final death rates (cf. Fig. 6).

Reliability of slicing. The effectivenesss of the slicing requires examination, since it underpins the ensuing analysis of the recovery cycle of the discharging motoneurone. Such analyses inevitably require some such filtering of the raw spike train since some fluctuation in central synaptic drive and mean firing rate is inescapable during a prolonged voluntary contraction, however well-trained the subject. The criteria for creating a homogeneous slice could easily have been extended, but no procedure can ever fully correct for such untoward changes. It seemed best to err on the side of simplicity and use just the mean firing rate measured over approximately 1 s.

The present determination of the mean firing rate is subject to two types of error that limit its reliability as a measure of the central synaptic drive acting upon the motoneurone, moment by moment. First, the drive will sometimes change in the course of the period over which it is being measured; the more slowly such changes occur, the less the error. Second, even when the drive is constant, the inherent variability of the interval distribution means that the measurements of drive will also be subject to statistical fluctuation; this must cause some spikes to be allocated to the wrong frequency band.

These errors cannot easily be quantified or corrected. However, three observations show that, on average, the slicing was separating genuine subpopulations of intervals with different levels of central drive. First, as shown in Fig. 4, the slicing regularly separated subpopulations with different interval distributions and mean frequencies. Second, when the mean frequency of a sliced subpopulation was compared with the mean value of the running mean for each of its constituent spikes, the values agreed closely (normally within 0·1 Hz); this would not occur if the variations in the running mean were simply due to random accumulations of the moment-to-moment variability of the interspike intervals. However, such statistical variation must have affected the slicing, and any deviations between the means tended to occur for slices whose drive was at one or other extreme of the population studied (the mean of the sliced subpopulation then lay very slightly closer towards the mean of the whole population than did the mean of its drive frequencies). Third, a significant positive correlation was regularly observed between the values of nearby interspike intervals when the first ten serial correlation coefficients were computed for the whole of the original population, confirming that the firing rate drifted during the recordings.

The correlation coefficients were usually in the range +0·1 to +0·3; the ten successive values tended to show a progressive slight decline. However, particularly for higher firing rates, the first coefficient was sometimes appreciably lower than the immediately subsequent values, suggesting that short intervals tended to be followed by long intervals, and vice versa. For example, in one extreme case the coefficients were 0·03, 0·24, 0·19, 0·19, 0·15, 0·15, 0·16, 0·16, 0·11 and 0·13 (biceps unit with 2891 spikes firing at 11·7 Hz), while in another case at the other extreme they were 0·37, 0·38, 0·33, 0·29, 0·30, 0·27, 0·26, 0·25, 0·25 and 0·23 (brachioradialis unit with 11 907 spikes firing at 11·1 Hz). In a more typical example, the coefficients were 0·25, 0·28, 0·23, 0·17, 0·19, 0·16, 0·16, 0·17, 0·17 and 0·13 (brachioradialis unit with 3406 spikes firing at 9·1 Hz). A frankly negative first coefficient has been occasionally seen by others (Person & Kudina, 1972; Kranz & Baumgartner, 1974) and attributed to the summation of the AHPs produced by successive spikes, as observed with intracellular recording (Ito & Oshima, 1962). This must have slightly influenced the slicing, but does not merit further consideration.

The trajectory of the motoneurone membrane potential during the interspike interval

At low firing rates, the interval death rate becomes constant, showing that the spikes are being triggered purely by synaptic noise rather than by a continued change in

membrane potential. Moreover, the membrane potential may be suspected as having become stabilized well below threshold; if it were above, the death rate would be very high and the interval histogram would end abruptly rather than in a gentle exponential decay. For subthreshold potentials, the closer the potential gets to threshold the greater becomes the probability that noise will trigger a spike in the next unit of time. For each particular noise level, there will be a one-to-one relation between the two variables, potential and probability; increasing the noise will lead to more excitation at a given potential. Given the appropriate relation, the potential, in millivolts, can be deduced from the interval death rate. Likewise, once an equation is obtained, the whole death rate plot can be transformed to give the trajectory of recovery of the membrane potential in the last part of the interspike interval. No analytical solution was available to provide the transform so it was determined by computer modelling, as described in the Appendix, with the result shown in Fig. 13. In essence, potential was obtained from probability

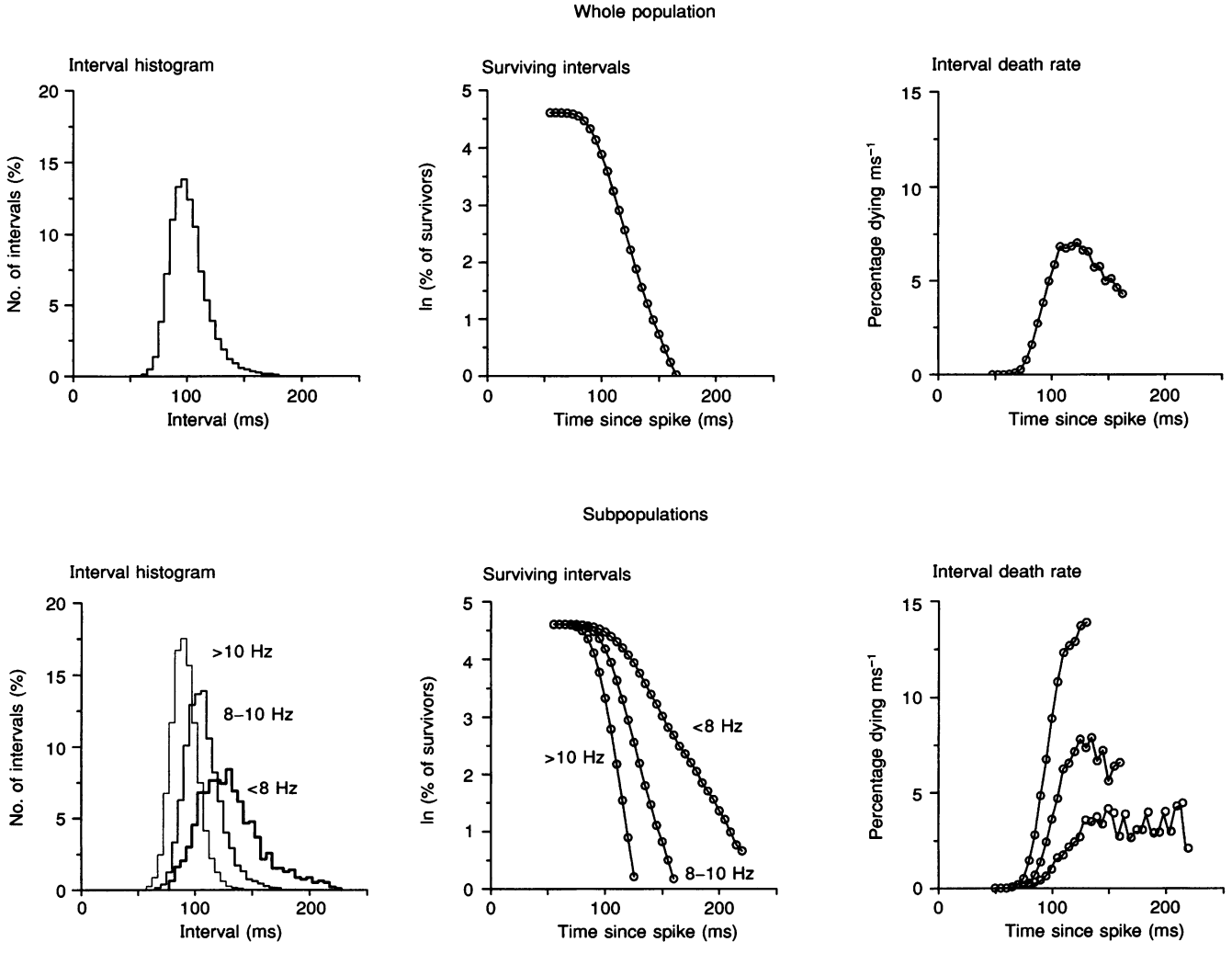

Figure 4. Subpopulations with different firing rates sliced from a single recording

The top plots, in the same format as Fig. 2, show the interval distribution for a brachioradialis motoneurone firing at an overall mean rate of 9·8 Hz. However, when measured second by second, the rate varied slightly during the recording. Three separate subpopulations of intervals were separated, depending upon the current short-term firing rate (above 10 Hz, 8–10 Hz, below 8 Hz). The bottom plots show their distributions; the differences parallel those seen in Fig. 3 on deliberately varying the firing rate, with the final death rate decreasing and the variability increasing with the reduction of firing rate. From left to right, the coefficients of variation of subpopulations were 13, 16 and 24%, respectively. The slight departure of the final part of the top distribution from an exponential (seen especially in the death rate) is attributed to its compounding slightly differing subdistributions. (The whole population comprised 19724 intervals after removing 36 stray intervals below 50 ms, or 0·2%; its mean firing rate was 9·8 Hz, with a coefficient of variation of 18%. The subpopulations had mean firing rates of 10·6, 9·3 and 7·6 Hz, and comprised 9346, 9452 and 926 intervals, respectively.)

by fitting a curve to the experimental points given by the model motoneurone; the sum of two exponentials was used since this provided a convenient arbitrary function for routine use. Since the level of synaptic noise is inevitably an unknown, the trajectory cannot be determined directly in millivolts; it was thus scaled in 'noise units', equal to the standard deviation of the on-going synaptic noise in millivolts. Moreover, all values have to be expressed relative to the firing threshold rather than to zero millivolts. The modelling used time-smoothed Gaussian noise, as found by Calvin & Stevens (1968) with intracellular recording, and took their value of 4 ms for the smoothing. This corresponds to the membrane time constant, and changing its value slightly changes the transform. The simplest possible model was used, with all variables expressed in terms of deviation of membrane potential from a constant

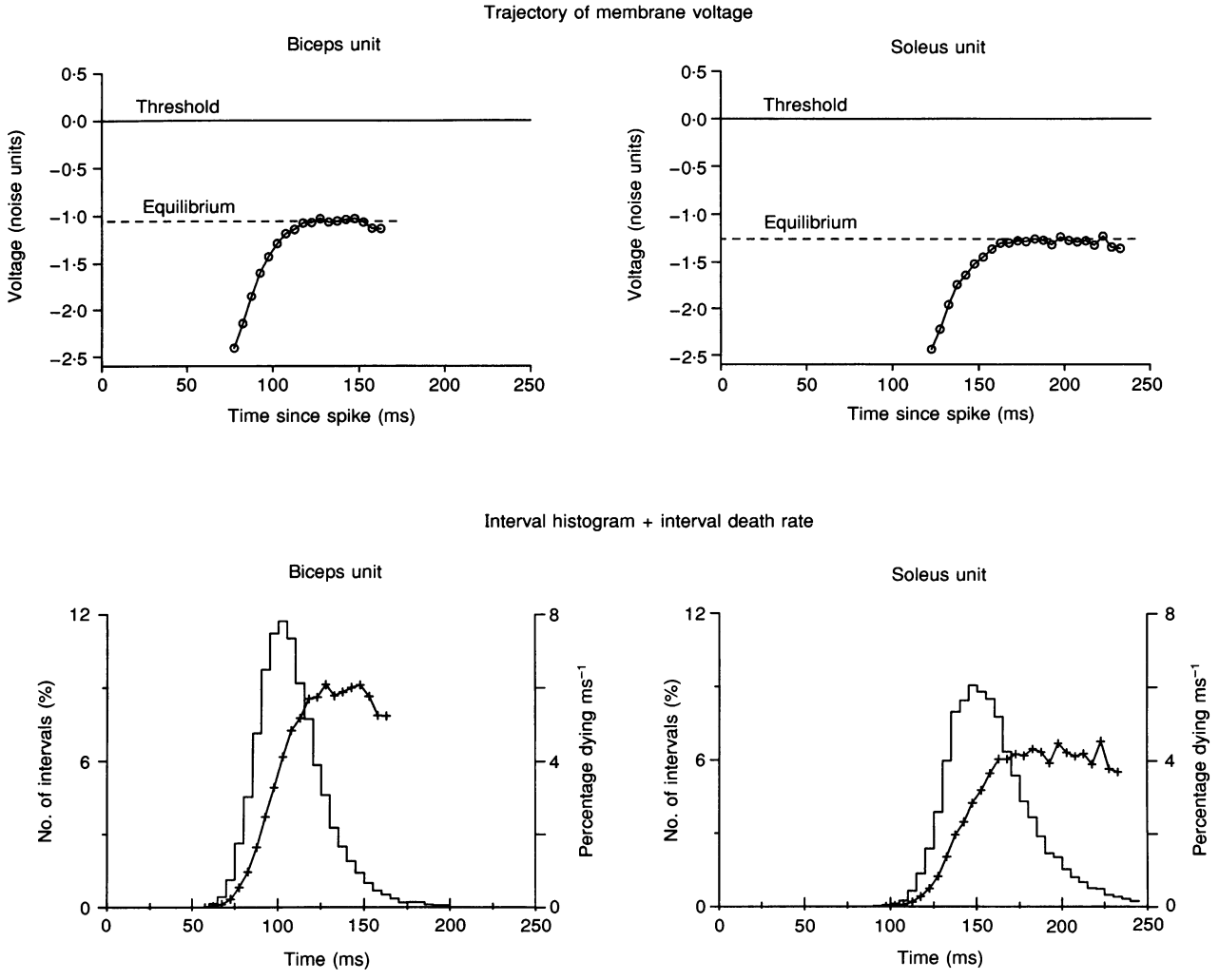

Figure 5. Post-spike membrane potential trajectories derived from interval histograms

The trajectories (top) were determined by applying the transform of Fig. 13 to the interval death rates shown below (+); this gives a value for the membrane potential scaled in terms of the standard deviation of the on-going synaptic noise (= 1 noise unit). The values are all referred to the threshold for spike initiation; negative values correspond to hyperpolarization. The motor units were firing near the bottom of their frequency range, with appreciable coefficients of variation (biceps, 20%; soleus, 17%). The trajectory of the post-spike AHP then decays to an equilibrium well below threshold. The biceps data are based on 16 933 intervals recorded while the unit was firing in the range 7·5–11 Hz and the soleus data are based on 27 085 intervals during firing at 5–7·5 Hz; these were sliced subpopulations comprising the majority of the original populations (85 and 89%, see Fig. 4). The slicing improved the homogeneity of the data by removing short periods of unduly low- or high-frequency firing; the mean frequencies of firing of the slices (9·2 and 6·2 Hz) were within 0·1 Hz of the original values. A negligible number of extraneous spikes were removed from the original populations (biceps, 2 below 50 ms or 0·01%; soleus, 165 below 80 ms or 0·5%). Voltages below −2·5 noise units were not determined, since the estimates became unreliable (corresponding death rates below 0·4%); the computation of the death rates, and thus of the trajectories, was terminated when the number of surviving intervals fell below 2% of the initial number.

threshold; membrane conductance changes and capacitance were ignored. The present 'physiologically' determined trajectories are thus potentially slightly distorted, as discussed later.

The top plots of Fig. 5 show such computed trajectories for two further motoneurones, again firing at the bottom of their frequency range. In each case, the potential traverses a smooth curve which comes to equilibrium slightly more than 1 noise standard deviation below threshold. The equilibrium potential may be presumed to correspond to the net potential resulting from the leak conductance that produces the resting potential and the effective synaptic currents that reach the soma. Moreover, the curves resemble the final decay of the AHP recorded intracellularly following a spike. The death rate plots, used to deduce the trajectories, are shown at the bottom of Fig. 5 and help illustrate the effects of the transform. The most relevant difference between the plots is that the top of the approximately linear ramp in the probability plots has been converted into a curve in the membrane potential trajectory; as the probability of a spike increases, the transform converts a given increment in probability into progressively smaller increases in potential. Likewise, the transform smooths out the noise in the plateau of the probability plot. This is all more simply expressed in terms of the real cause and effect relation, namely that between the membrane potential and the probability of firing. The closer the potential gets to threshold, the more rapidly the probability increases (corresponding to the rising limb of a Gaussian distribution), and a given change in potential produces an ever larger increase in probability.

Distortion of trajectory on mixing disparate populations

The precise curvature of the last part of a trajectory estimated from the interval data can be considerably influenced by any admixture of populations with different mean frequencies. This is important, because it affects the numerical values required to fit an equation to a trajectory for comparison with real AHPs. The nature of the distortion must be considered in detail so as to establish which parts of the trajectory can be relied upon, and which parts discounted; without this, analysis of the AHP becomes impossible. Some admixture will always be present for human recordings, even after slicing a spike train into components with different firing rates.

The distortion is illustrated in Fig. 6; its principal feature is a sharpening of the angle of approach of the trajectory to its final equilibrium, as shown by the curve joining the open circles, bottom right. For clarity of illustration the 'pure' populations of intervals were synthesized by using a model motoneurone with an exponential trajectory (see later), but the distortions occur equally for natural populations of intervals. Subpopulations for different firing rates will then shade into each other, and a slice for a given frequency will be contaminated by outliers from either side. In essence, in the presence of a limited amount of 'contamination' of a population by those of other frequencies, the initial rising phase of the trajectory remains a reasonable indicator of the form of the AHP, while a sharp curve preceding the final plateau is potentially misleading. Moreover, any sag of the trajectory from an initial peak is probably artefactual, and also any short plateau following an abrupt angulation. However, a plateau in the death rate plots for relatively impure populations like those of Figs 1–4 is meaningful, and does show that during low-frequency firing the membrane potential comes to equilibrium well below spike threshold. The precise level measured will be that for the lowest frequency periods of discharge, and any periods of discharge at high frequency will have been without effect on this portion of the trajectory. A fuller description is given below.

The distortion explained. The plots on the left of Fig. 6 show the data for the two pure subpopulations with different mean frequencies, which were mixed; the trajectories were computed from the histograms with the usual transform, which successfully recovered the exponentials used as the starting point. The thick plots on the right show the properties of the impure population produced by amalgamating the two subpopulations. It is matched against a pure population of similar frequency (which was actually chosen so that its trajectory had an equilibrium value halfway between those of the two subpopulations). The mixed histogram starts before the one for the pure population and ends later; this is to be expected, since it contains both an excess of short intervals derived from the 9·8 Hz subpopulation, and an excess of long intervals from the 7 Hz subpopulation.

The mixed trajectory reflects its origins and differs from its companion pure curve in three principal ways: first, it starts slightly earlier; second, it comes to a lower final equilibrium; third, the smooth exponential of the individual distributions is transmuted into a much sharper curve and the final equilibrium appears to be stably achieved much earlier. With subpopulations of more widely separated frequency, the mixed trajectory sags back from an initial peak as in Fig. 4, and may approach a final equilibrium from above. In all such compounding of disparate populations, the initial part of the mixed trajectory largely reflects that of the high-frequency subpopulation, while its final tail approximates to that of the low-frequency subpopulation. The sharp curve of the mixed trajectory occurs as the relative importance of the contributions from the two subpopulations becomes reversed.

There is a major difference in the contributions provided by the two subpopulations, which prevents the mixed trajectory being simply an arithmetic mean of the two original trajectories; it arises because computation of the interval death rate (and with it the trajectory) depends only on the survivors at a given interval since a spike. The rising phase of the trajectory is relatively close to a weighted arithmetic mean of the subtrajectories (all intervals contribute to its determination, with most deaths from the high-frequency population), but the final part of the mixed trajectory is virtually the same as the low-frequency trajectory (since nearly all

the long intervals came from the low-frequency subpopulation). In Fig. 6, for example, the mixed trajectory comes to the same equilibrium as the 7 Hz trajectory. In the example shown, the two initial populations contained the same number of impulses. The same principles apply when a pure population is contaminated by a smaller number of outliers from populations with different firing rates; again, the curvature of the trajectory tends to be sharpened and there may be a short plateau lying well below that for the main population.

Trajectories for different firing rates

Figure 7 shows a systematic analysis of the effect of the firing rate on the form of the trajectory for a pair of motoneurones that could be studied in particular detail, with over 90 000 spikes recorded from each. The different firing rates were obtained by a combination of varying the level of voluntary drive and slicing the resulting populations of different frequency into further subpopulations, as detailed in the legend; Fig. 5 shows part of the same data without significant slicing. The individual trajectories were terminated when they became irregular or if they began to sag, since this was probably due to residual contamination of the purity of the slice (see above). The underlying interval histogram was normally over 95% complete when a trajectory was terminated, so only a very small part of its final tail was ignored. The short stubs at the end of some of the trajectories remain somewhat suspect; much greater

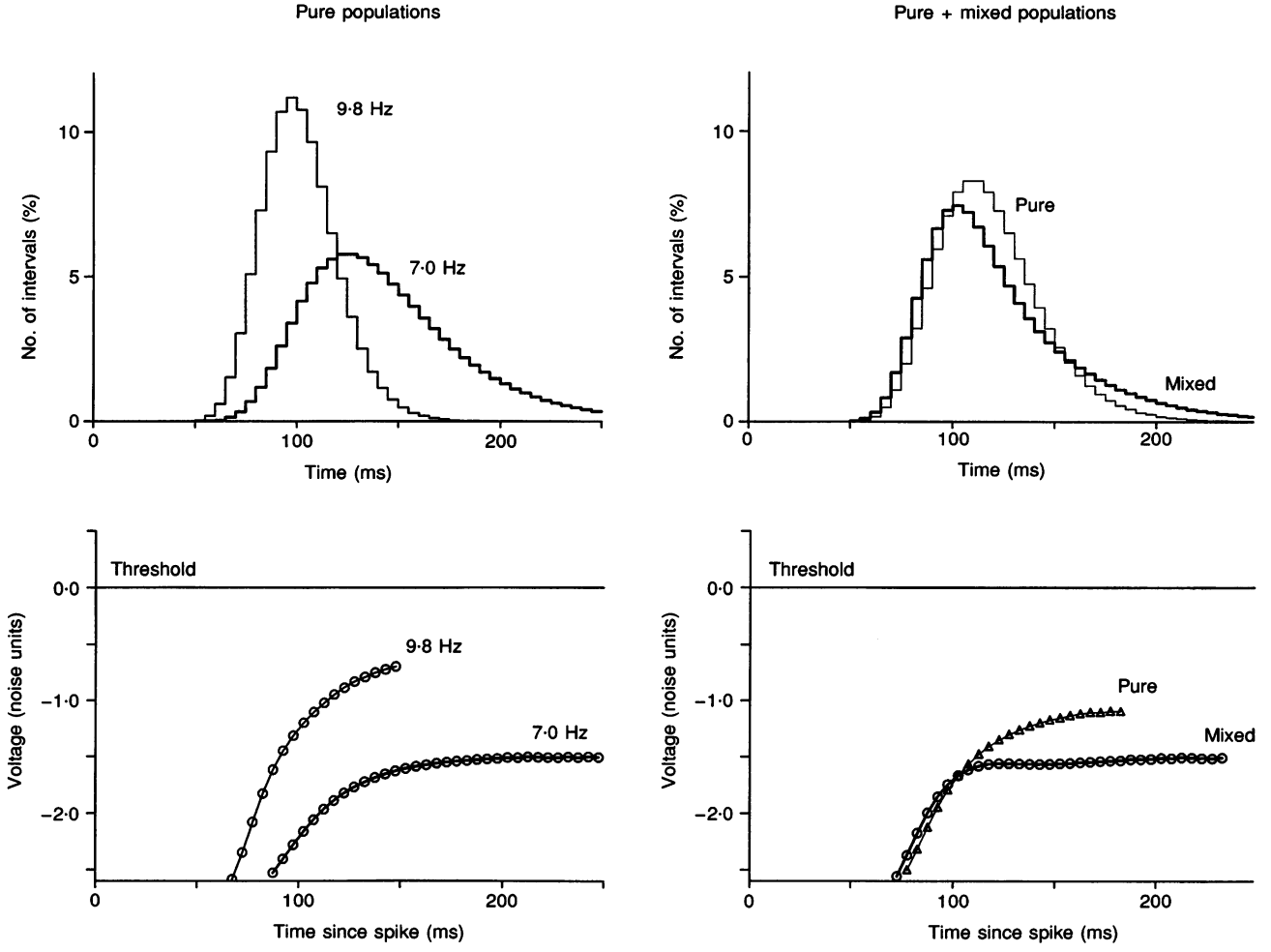

Figure 6. Effect of mixing populations with different means

Top, interval histograms for 4 separate populations of intervals. Bottom, their underlying trajectories, determined as for Fig. 5 from the interval histograms. The mixed population on the right was obtained by combining the two pure populations of intervals shown on the left; the pure population on the right has approximately the same mean firing rate as the mixed population (8·4 *vs.* 8·1 Hz). The trajectory of the mixed population reached its final equilibrium more rapidly than those of the pure populations, which all approached it exponentially. The flattening and other differences have been highlighted by using synthetic populations of intervals (computed as in Fig. 11); mixing natural populations had similar effects. (The parameters of the model were the same as in Fig. 11; the levels of drive for the pure populations were −0·5, −1·0 and −1·5 noise units. From left to right, the means of the interval histograms were 102, 144, 123 and 119 ms with coefficients of variation of 18, 27, 30 and 22%. The trajectories end when 98% of the intervals have occurred.)

reliance can be placed on the shape of the rising phase, since far more spikes contributed to its determination.

Both units showed the same typical changes in the shape of the trajectory as the mean firing rate increased, but on a different absolute time scale. When the unit was firing at the bottom of its range, the trajectory came up to a long plateau, stabilizing well below threshold as in Fig. 5. As the firing rate increased the plateau became shorter and lay closer to threshold, while the initial part of the trajectory became appreciably steeper as well as starting somewhat earlier (i.e. reaching the threshold for detection of approximately 2·6 noise units). At the highest frequencies, a clear plateau never developed and the trajectory terminated in the region of threshold. It should be noted, however, that a potential plateau near, and especially above, threshold would normally be unable to display itself, because the underlying probability of firing becomes so high that virtually all intervals would have been terminated by a spike appreciably earlier; to obtain a reasonable number of long intervals against huge statistical odds would require an unduly long recording, and any plateau would be greatly at risk of distortion by a small degree of admixture with lower-frequency discharges. What matters is that the main part of the trajectory invariably became steeper with increase in firing rate, since this has been a matter of debate (Nordstrom *et al.* 1992; Warren *et al.* 1993); moreover, this could not have been produced artefactually by any residual mixing of populations with different firing rates.

Estimating the AHP by combining the individual trajectories

Figure 8 combines the trajectories of Fig. 7 to provide an estimate of the last part of the AHPs of the two motoneurones. These compound trajectories have been produced by shifting the individual trajectories vertically along the voltage axis so as to superimpose them upon a common curve; attention was focused on their rising phases, since these are least prone to error. The various trajectories then

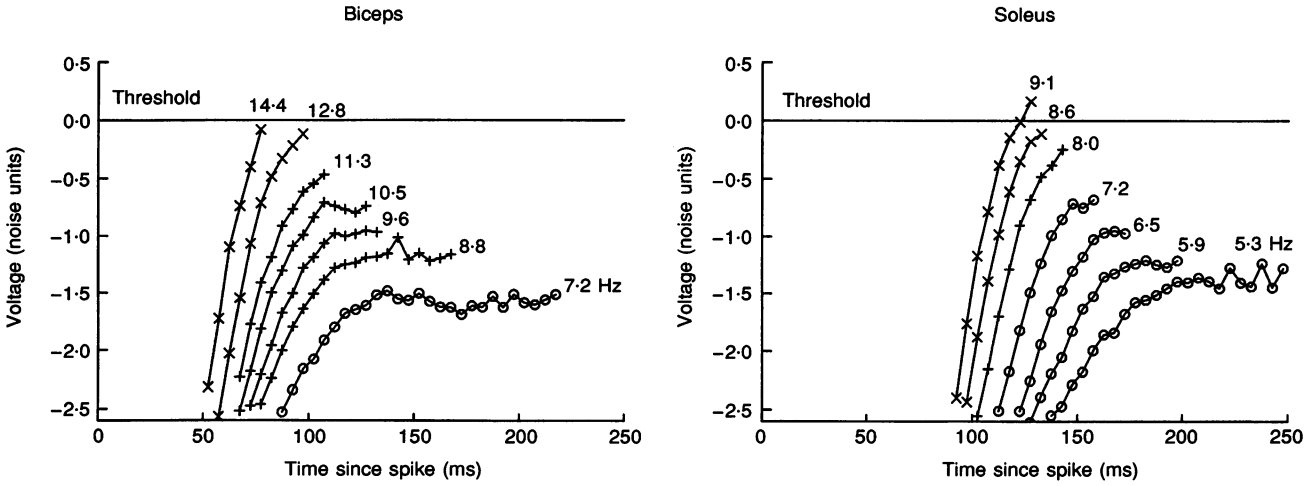

Figure 7. Family of trajectories for different firing rates

The trajectory of the post-spike membrane voltage was determined, as in Fig. 5, for a series of subpopulations with different on-going mean frequencies of firing (value in Hz shown next to each trajectory). The higher the frequency, the steeper the initial part of the trajectory and the shorter and higher any period of final equilibrium. The range of frequencies was obtained partly by varying the level of voluntary drive to produce 3 separate populations of intervals for each unit, with different mean firing rates (separate symbols); these were then subdivided according to the on-going mean firing rate, measured second by second as in Fig. 4 (comparable subpopulations for the different levels of voluntary drive were very similar, but were not combined). The absolute value of a noise unit in millivolts was probably slightly different for each trajectory, but without affecting the overall picture. The original populations had mean rates of 12·5, 10·1 and 8·8 Hz for biceps and of 8·0, 7·5 and 6·3 Hz for soleus; the proportion of stray spikes that had to be removed increased with the firing frequency of each unit (values of 0·04, 1·5 and 6·4% for biceps; 0·5, 0·7 and 3·3% for soleus). All trajectories were based on over 4000 intervals, after strays removed, except for those for 14·4 Hz for biceps ($n = 1963$) and for 9·1 Hz for soleus ($n = 3336$); *in toto*, the trajectories shown use the measurements on 41 682 intervals for biceps and 47 629 intervals for soleus. Each trajectory includes data for on-going frequencies spanning a range of about 1 Hz, without overlap (the ranges, expressed as an interval in milliseconds, were 60–70, 75–80, 80–90, 90–100, 100–110, 110–130 and 130–165 for biceps, and 100–112, 112–120, 120–130, 130–145, 145–160, 160–180 and 180–220 for soleus). Eleven of the 14 trajectories plotted used over 95% of the spikes in their subpopulation before being terminated. The remaining 3 used just over 90% (plots for 5·9, 6·5 and 14·4 Hz); they were shortened because they began to sag (cf. Figs 4 and 6). Same units as in Fig. 5.

fell remarkably well into register, providing an empirical demonstration that they represent overlapping segments taken from a more fundamental basic trajectory and then displaced by varied amounts. Shifting them along the horizontal axis does not produce effective superposition, merely a fan of separate curves. The basic curve underlying the compound trajectory is suggested as corresponding to the waveform of the AHP of the motoneurone. Explanation of this hypothesis, together with the rationale for the vertical shift, provide an essential prelude to further analysis of the data.

The locus and shape of each of the individual trajectories of Fig. 7 will depend both upon the level of synaptic drive, which will increase progressively with firing rate, and upon the time course of the underlying AHP, which should be invariant for each unit. If the situation is simplified by ignoring the conductances and assuming linear summation of voltages, then each trajectory is simply the sum of the mean synaptic depolarization and the AHP; every trajectory will then reproduce the form of the AHP, but at a different vertical locus. However, any one individual trajectory obtained by interval analysis will only display a short segment of the full AHP, different for each firing rate, since each interval histogram spans a limited range. Initially, the membrane potential is too far from threshold for the noise to trigger spikes, and no information is obtained; next, the potential comes within range of threshold, noise-induced firing occurs and the trajectory can be determined; finally, as threshold is neared, the noise will have excited a spike on almost every occasion and the trajectory is terminated, even though the motoneurone has not fully recovered and the AHP remains incomplete. Thus an appreciable part of the AHP can be estimated by superimposing the individual trajectories after shifting them vertically; the range spanned is then much greater than for an individual trajectory. This also assumes that the absolute size of the noise unit remains approximately constant with the changing drive (see Appendix).

The amount by which each trajectory requires to be shifted corresponds to the mean depolarization produced by the synaptic drive associated with the trajectory; each trajectory is based on a period of discharge with a different firing rate and a different underlying synaptic drive. The initial rapidly rising phase of the AHP is derived from slices with a high firing rate associated with considerable depolarization; the final gentle curve is based on slices with a low firing rate and relatively weak synaptic depolarization. Estimated this way, the synaptic depolarization differed by 3–4 noise units between the extreme trajectories of Fig. 7. The individual values are plotted in Fig. 12.

Shape of curve. The curve fitted to the estimated AHPs is a simple exponential. It provides a close fit to the points for the rapid rising phase of each of the individual trajectories;

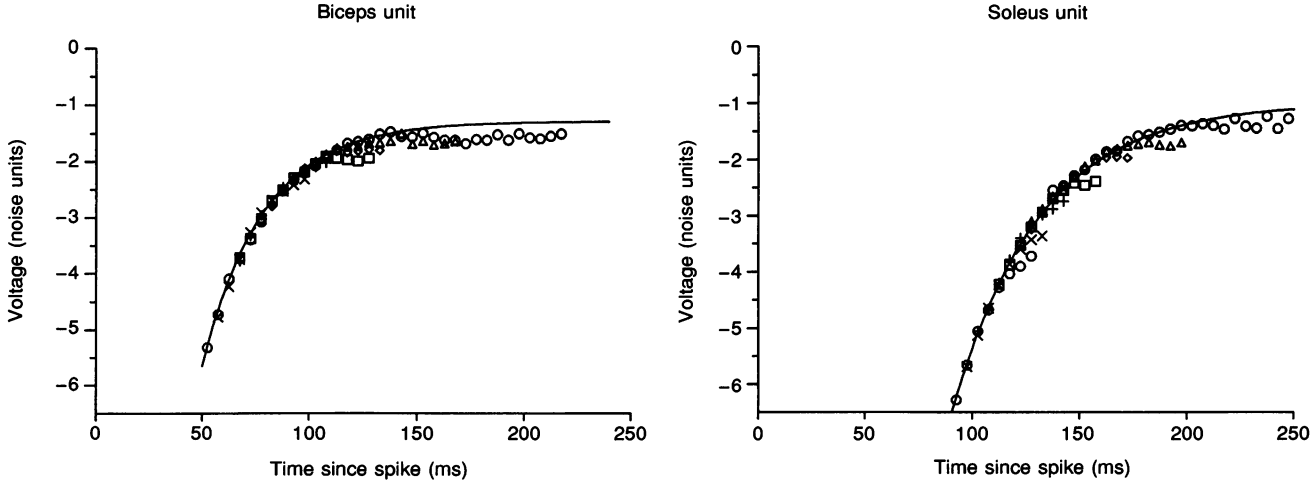

Figure 8. Compound trajectories representing AHPs produced by combining a family of individual trajectories

The trajectories of Fig. 7 have been compounded to give a fuller estimate of the time course of the post-spike AHP of each motor unit. Taking the lowest trajectory as the reference, the next upwards trajectory was shifted down, along the voltage axis, until the rising parts of the two trajectories superimposed. The superimposed pair then became the new reference and the next trajectory was shifted into correspondence, and so on. This is suggested as corresponding to adding a hyperpolarization to each individual trajectory and so counteracting the depolarization produced by the greater synaptic drive responsible for increasing the firing rate; it is assumed that the absolute value of the noise unit remains approximately constant. Each individual trajectory has a separate symbol, except for those at the two extremes; every original point has been included. The curves are simple exponentials; their equilibrium value is deliberately slightly above the experimental points for long intervals (cf. Fig. 6). The time constant is longer for soleus than for biceps (41 *vs.* 29 ms).

this is their most meaningful portion since it is least affected by any inhomogeneity in the underlying population of intervals. An exponential was used for two quite different reasons. First, it provided a good empirical fit to the data. Second, it is theoretically appropriate because the increased conductance responsible for the AHP decays exponentially (Kernell, 1968).

The last few points of several of the trajectories fall below the curve. This is likely to have been due to a slight residual inhomogeneity, and so has been neglected. Likewise, the terminal part of the lowest-frequency trajectory for each unit (○) was also discounted, and the exponential allowed to come to equilibrium at a slightly higher level in accordance with the shape of the earlier part of the compound trajectory. This compensates for the type of distortion shown in grosser form in Fig. 6. (The exponential was fitted to the data with an optimizing procedure which varied each of its three parameters – starting level, time constant, final level – and ignored the final tail.)

Comparison of AHPs of different motor units

The AHPs of the two units of Fig. 8 differ markedly in their time course; the soleus AHP is an approximate version of the biceps AHP, but delayed by some 50 ms. The parameters of the fitted exponential provide a convenient way of characterizing the AHPs more fully. The final equilibrium values shown in Fig. 8 have no significance; they simply depend upon the lowest firing rate that happened to be studied, since it was this which provided the reference for shifting the other trajectories. As a description of the AHP, the curve has to be bodily shifted to come to equilibrium at zero. The two remaining parameters are the time constant and the initial amplitude; both were greater for the soleus unit, with completely different types of implication (time constants, 29 and 41 ms; amplitudes, 24 and 50 noise units). The time constant can be taken to be that of the underlying conductance change; this is known to be exponential, with a time constant varying between motoneurones (Baldissera & Gustafsson, 1974*a*). The amplitude, however, is measured in noise units, not millivolts, and the difference between the two motor units seems more likely to be due to a difference in their synaptic noise rather than in the absolute size of their AHPs; the measurements thus suggest that the biceps unit had appreciably more synaptic noise than the soleus unit. It should immediately be emphasized that the amplitude measurement is relatively inaccurate; a small error in the value of the time constant is associated with a relatively large error in the value of the amplitude, since an exponential relation is being fitted to the data and there are no points near the origin. When the time constant is falsely taken to be slightly below its true value (as from a slight artefactual sharpening of the curvature of the trajectory), then the amplitude of the AHP becomes unduly large to enable the curve to fit the measured points.

Figure 9 shows the range of the AHPs observed, estimated in the same way as those in Fig. 8; each has been fitted with an exponential, and shifted vertically to bring the equilibrium to zero. With one exception (right-hand graph; FDI, ●) they form a single family of curves moving progressively to the right, with an approximately regular increase in their time constants in the range 20–40 ms and with comparable initial values in the range 30–100 noise units (see legend). Their progression is emphasized more by their lack of overlap than by the precise numerical values of their two parameters, which may be mutually in error. Such consistency between units confirms that the trajectories extracted by the present analysis are physiologically significant, and reflect meaningful features of the interval distribution.

The exceptionally flat trajectory in Fig. 9 (right-hand graph) had a very long time constant (50 ms) and a very small initial value (8 noise units); this suggests that it was for a small, slow motoneurone with a very high level of synaptic noise. One other flat trajectory was observed among the twenty-one further compound trajectories obtained by superimposing the individual trajectories of other motoneurones; these otherwise lay close to one or other of those already shown. It was for the only ADM motor unit studied (time constant, 36 ms; initial size, 12 noise units). Both the unusual motoneurones supplied intrinsic hand muscles, whose motoneurones are thought to receive a particularly powerful input from individual corticospinal fibres; this may have been responsible for their high noise level, but very high levels were not invariable for such motoneurones – four other FDI motoneurones had typical trajectories (cf. Fig. 9; left-hand graph, □). In contrast, soleus motoneurones tended to have rather low noise levels as judged by their AHPs, being relatively large when expressed in noise units (Fig. 8 values, 74 and 97 noise units). This might reflect a paucity of corticomotoneuronal input. More importantly, the time constant for soleus motoneurones was regularly greater than average, as in Fig. 9.

Discharge variability of motoneurones with different AHPs firing at the same rate

In mathematical terms, the trajectory deduced from the spike discharge is simply a transformation of the interval histogram data and displays the same information in condensed form. Thus, for any given mean frequency of firing, units with similar AHPs and noise levels should produce similar interval histograms, as was regularly observed. In contrast, the fine patterning of the discharge should be quite different when motoneurones with different AHPs happened to be firing at the same mean rate. Figure 10 extends earlier observations (Tokizane & Shimazu, 1964) showing that there is no one standard interval histogram for a given firing rate applicable to all motoneurones.

The first three pairs of histograms in Fig. 10 are for the two units whose rather different AHPs are shown in Fig. 8; both fired part of the time at about 8 Hz, so suitable populations for comparison could be selected by slicing. The soleus unit was being excited early in its AHP, so showed

rather little variability; in contrast, the biceps unit was being excited at the end of its AHP and the variability was high. When the soleus unit was firing at 8·5 Hz, the mode of its histogram was approximately the same as that for the biceps unit firing at 8·0 Hz. When their mean firing was matched, the soleus modal value was the greater. In both cases, in comparison with the soleus unit, the biceps unit fired an excess of both short and long intervals and the coefficient of variation of its discharge was twice as great. However, when biceps was driven to fire early in its AHP, its discharge variability decreased, and when soleus was excited late in its AHP, its variability increased; the relative values of their coefficients of variation were then reversed. The final pair of histograms compares the soleus unit with the one unit from ADM noted above; again, the soleus unit shows much less variability. Detailed examination of the trajectories for these various units showed that the similarities between the two sets of comparisons arose for different reasons. The biceps unit fired less regularly than the soleus unit largely because the time constant of its AHP was shorter, while the ADM unit fired so irregularly largely because it had a very high level of synaptic noise. This emphasizes that highly variable discharges occur through some combination of the firing rate being low enough for the AHP to be largely complete, and the noise level being high enough to bring an appreciable part of the trajectory within range of threshold.

Interval histograms for an exponential trajectory

The calibration between probability and voltage used above can equally be run in reverse from voltage to probability, starting with a truly exponential trajectory and finishing with an interval histogram. This both supports the earlier analysis and shows how variations in the noise and the AHP affect the histogram's shape. Figure 11 displays a series of such synthetic histograms for a motoneurone subjected to successively less synaptic drive, together with the strictly exponential trajectories used as the input. The histograms closely resemble those for real motor units. In particular, the histograms develop a tail and become much more positively skewed as the mean firing rate decreases. Their standard deviation also obviously increases. Figure 11 also emphasizes that each histogram derives from a variable segment of the full AHP (shown as a continuous line). At shorter times, the membrane potential is too far from threshold for the noise fluctuations to be able to trigger a spike. At longer times (shown as a dashed line), the trajectory potentially continues with the AHP unfinished, but the histogram is complete as the cumulative probability of a spike having been discharged verges on 100%.

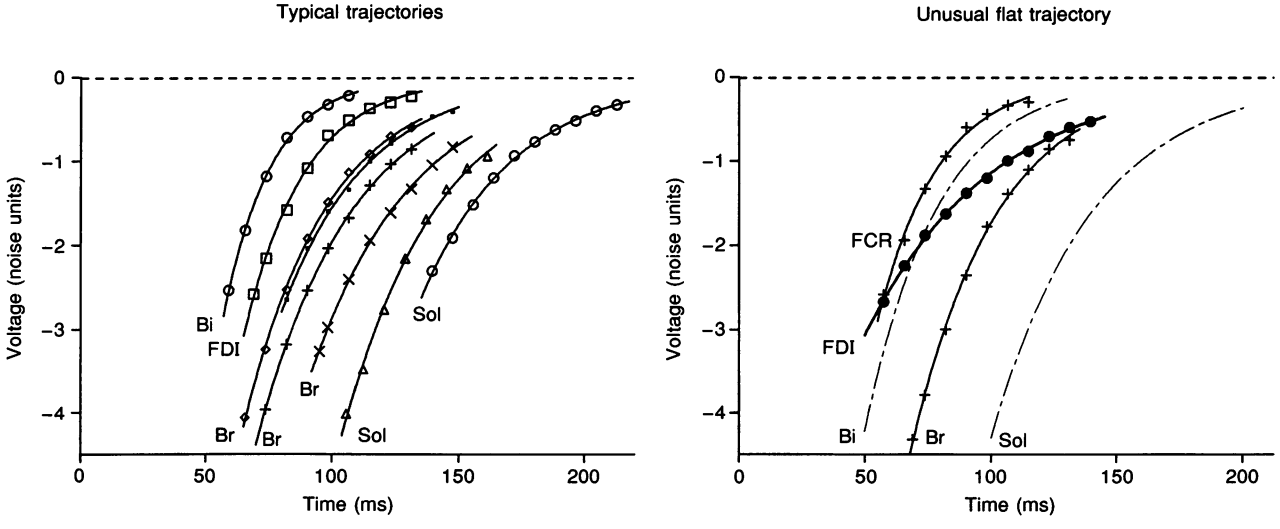

Figure 9. AHPs for a range of motor units

Each curve shows the last part of the AHP of a separate motor unit, estimated as in Fig. 8 and labelled with its muscle of origin. With one exception (right-hand graph, FDI), they form a regular series moving progressively to the right, and with their time constants tending to decrease. Bi, biceps; FDI, first dorsal interosseus; Br, brachioradialis; TA, tibialis anterior; Sol, soleus; FCR, flexor carpi radialis. Dashed lines, curves of Fig. 8. Each of the 3 Br units on the left came from a different subject. The points were obtained by measuring tracings of compound trajectories, derived by superimposing trajectories for subpopulations with different mean frequencies. Each set of points was fitted with an exponential curve; both curve and data were then shifted vertically to bring the final equilibrium to zero. From left to right, the time constants for the two sets of data were 19, 24, 33, 34, 37, 39, 36 and 37 ms and 50, 24 and 34 ms (Fig. 8 values, 29 and 41 ms). The initial size of the AHPs were 60, 47, 30, 29, 36, 74 and 97 for the first set and 8, 29 and 33 for the second set, and 24 and 50 for the dashed curves (values in noise units). The illustrated AHPs are based on 6800–71 000 spikes (median value, 16 000; strays removed). Almost all the subpopulations used contained over 1000 spikes.

Assumptions. Four major simplifications are involved in this modelling, paralleling those used in the Appendix to determine the transform (essentially they all involve treating the signals as voltages and ignoring the underlying conductances); for the limited part of the AHP studied, these seem likely to approximate to the complex real-life situation. First, the central drive exciting the motoneurone simply produces a fixed depolarization, so that increasing the level of drive can be simulated by shifting the membrane trajectory of the motoneurone vertically. Second, the basic trajectory of the post-spike AHP is simulated by a voltage that is independent of the depolarization; the slow underlying potassium conductance is unaffected by the voltage (Baldissera & Gustafsson, 1974*a*). Third, in the range studied, the AHP declines exponentially with time, as does the underlying conductance (Kernell, 1968; Gustafsson & Baldissera, 1974*a*) and there is no summation between successive AHPs. Fourth, the noise remains constant throughout, independent of the level of synaptic drive or the stage of the AHP.

Quantitative comparisons. Figure 12 summarizes the effect on the synthetic histograms of varying the two parameters of the model motoneurone, namely the amount of synaptic noise and the duration of the AHP. The 'standard' curve on the top left shows the progressive increase of interval variability with increasing mean interval for a motoneurone with an AHP time constant of 30 ms (approximately 120 ms total duration; Kernell, 1968) and a medium amount of noise (see legend). The two other curves show that for any given mean interval, the variability increased both when the noise was increased and when the duration of the AHP was reduced (noise increased by a factor of 2·5, AHP shortened to 20 ms). On average these produced fairly similar increases over the range examined, but the curves crossed, showing that the underlying relations differed. Thus, real motoneurones whose interval histograms match over a range of firing rates should have both the same AHP and the same level of synaptic noise, suggesting that they are similar both in themselves and in the type of input they receive.

The continuous curves in the top right graph of Fig. 12 are for the same three model motoneurones and show the way in which the mean firing rate increases with the underlying synaptic drive, expressed as a depolarization measured in noise units. In all three cases, the relation was fairly closely linear over most of the range examined, namely for drives bringing the equilibrium depolarization to somewhere near threshold (the slight departures at low frequencies are partly genuine and partly due to an arbitrary cut-off of 300 ms for the maximum interval allowed; this was done to

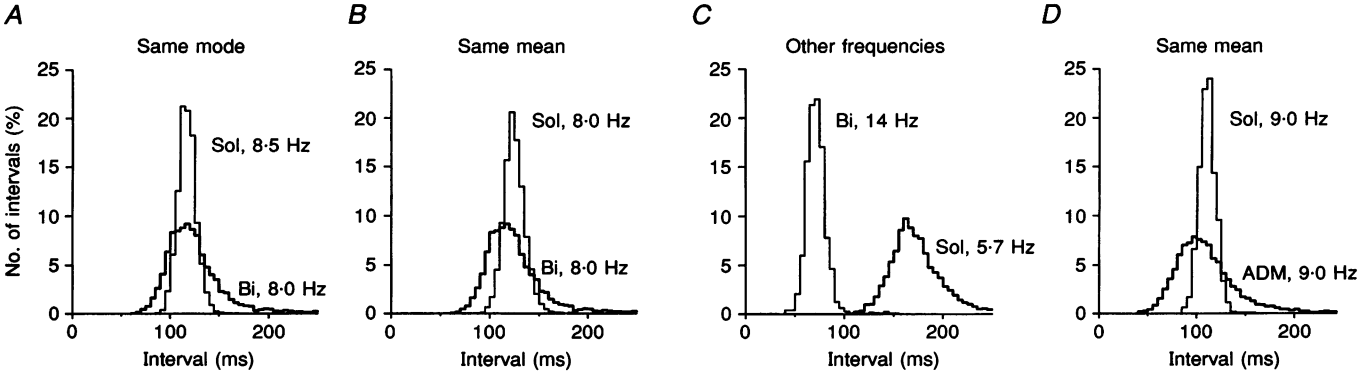

Figure 10. Interval histograms for motor units firing at the same mean rate but with different AHPs

The first three sets of histograms are for the pair of units whose AHPs are shown in Fig. 8. Subpopulations of intervals were used, for periods with an appropriate short-term on-going firing rate. In *A*, the peaks of the histograms come at nearly the same place (approximately equal modal values); the biceps unit produced more short intervals even though it was firing at a lower mean frequency. In *B*, the mean rate for soleus matches that for biceps; however, the histogram of biceps spreads further in both directions (coefficients of variation, 30% and 13%). The differences can be attributed to soleus having a slower AHP. *C* confirms that such differential patterning of the discharge was not, *per se*, a fundamental difference between the two motor units or their inputs, since the shapes of their histograms were reversed when the frequency was increased for biceps and reduced for soleus (coefficients of variation, 15 and 28%). *D* shows the same effects as *B* (coefficients of variation, 30 and 10% for the same mean firing rate), but with the soleus unit compared with one in ADM (same unit as in Fig. 1). In this case, there was probably an appreciable difference in the levels of synaptic noise, since the time constant of the AHP of the ADM was only slightly shorter (36 *vs.* 41 ms), while its initial amplitude was considerably smaller (12 *vs.* 50 noise units). All histograms are based on subpopulations with more than 3800 intervals (strays removed), except that of biceps at 14 Hz ($n = 1615$); the parent populations contained 25000–32000 spikes. The on-going firing rate for each subpopulation covered a range corresponding to 10 ms in its reciprocal, the mean interval for 10 adjacent intervals.

match the experimental data and produced a corresponding effect in the variation plots). Once again, increasing the noise and shortening the AHP had the same general effect, namely increasing the firing rate produced by a given mean synaptic drive, but, as with variability, the effects of changing the two parameters were not precisely equivalent.

The comparison of the three continuous curves on the right-hand side of Fig. 12 is complicated by the fact that the synaptic drive is expressed in the noise units for each particular motoneurone. Direct comparison is straightforward between the standard and shorter AHP curves since the noise is unchanged; their abscissae therefore have the same absolute scaling in millivolts. In contrast, each noise unit for the 'more noise' curve corresponds to a larger absolute potential. The dotted line rescales its central region in terms of the noise units for the standard lower noise level, bringing it onto the same absolute scale as the two other examples. This shows that increasing the noise increased the firing rate produced by a given level of synaptic depolarization (or current), with the relation differing from that found on shortening the AHP.

Comparison with particular motoneurones. The modelling shows that the precise relation between variability and firing rate, and between firing rate and synaptic drive, will vary from motoneurone to motoneurone. Real and simulated data were therefore compared. This showed that the experimental data for any given motor unit lay close to the curves given by a model motoneurone, with the values of noise and AHP that had been deduced for the real motoneurone. This is shown at the bottom of Fig. 12 for the two extensively studied units of Figs 7 and 8 (same spike trains used throughout). The agreement between the observed and predicted patterns of variability is of particular interest, because the standard deviations of the original interval histograms made no direct contribution to the determination of the AHPs used for the modelling. Similar comparisons were made for the eleven other units of Fig. 8, when the experimental values again lay close to the appropriate curves predicted by the modelling, which again covered a

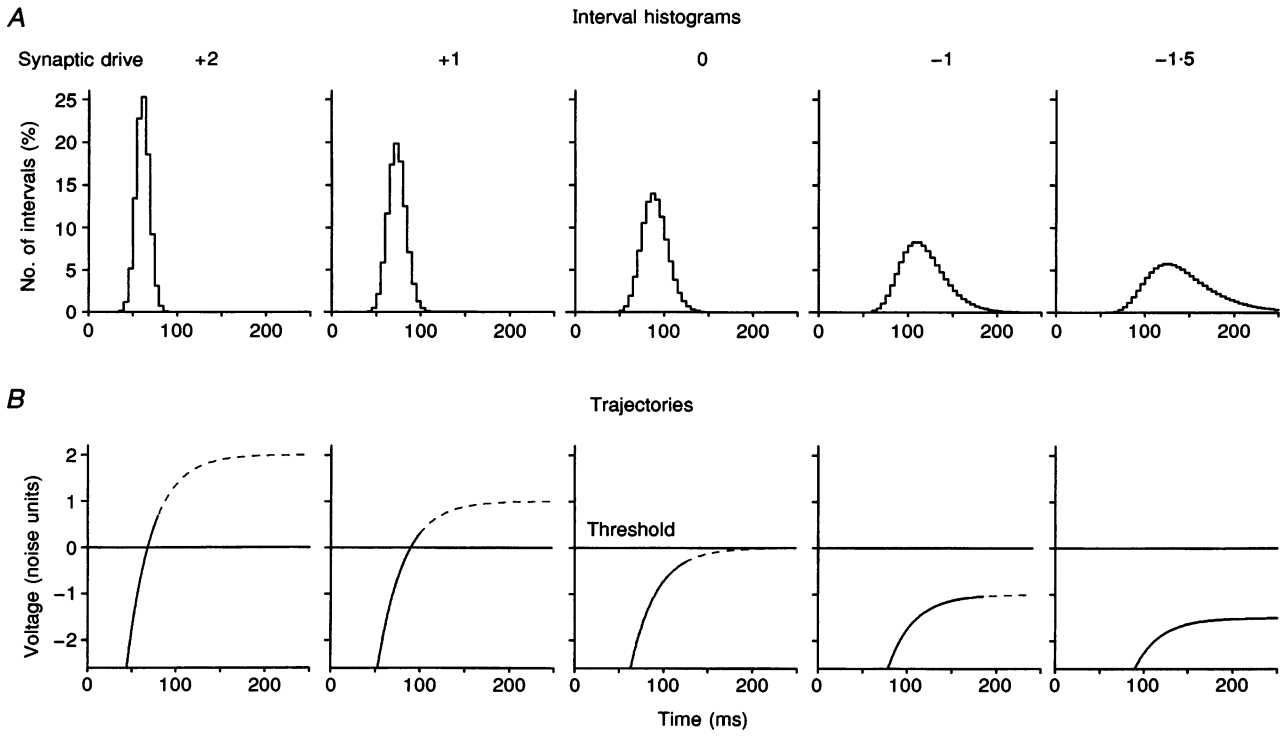

Figure 11. Interval histograms for a model motoneurone with the synaptic drive varied

The model had an exponentially decaying AHP which summed linearly with the synaptic drive to give the mean membrane potential trajectories shown below. As the drive decreased, the mean interval increased and the histogram broadened and became skewed (the coefficient of variation was successively 13, 14, 16, 22 and 28%; the skew increased from close to zero to +0·8 for the last 2 histograms). The dashed portions of the trajectories did not affect the firing pattern, since the histograms were then complete, with an insignificant number of spikes at these intervals. The potential is scaled in terms of the the standard deviation of the synaptic noise (1 noise unit), with zero corresponding to threshold for spike initiation; the depolarizing drive is in the same noise units, with zero corresponding to the mean excitation required to bring the final equilibrium potential to threshold. The histograms were computed by using the Gaussian transform of Fig. 13 to convert the voltage shown in the lower graphs into the probability of an on-going interval being terminated by a spike in the next millisecond, then performing serial calculations from zero to determine the number of spikes discharged at each time. The AHP of the model was set to match that of the biceps unit of Fig. 8.

wide range of behaviour. It is concluded that, in spite of its simplifications, the present model of motoneurone firing combining the AHP with synaptic noise, provides a remarkably satisfactory explanation of the varied shape of the interval histogram.

In making the above comparisons, the observed coefficients of variation normally lay further above the curves than those of Fig. 12; for any given unit, the deviation tended to increase with the mean interval. An average value for this deviation was obtained by taking the central value for each unit, in the middle of its firing range, and then averaging across the eleven units. The mean upward displacement of the experimental points corresponded to a coefficient of variation of $3{\cdot}7 \pm 1{\cdot}1\%$ (means $\pm$ S.D.). Some such discrepancy is to be expected, since the synaptic drive will have varied slightly during collection of the

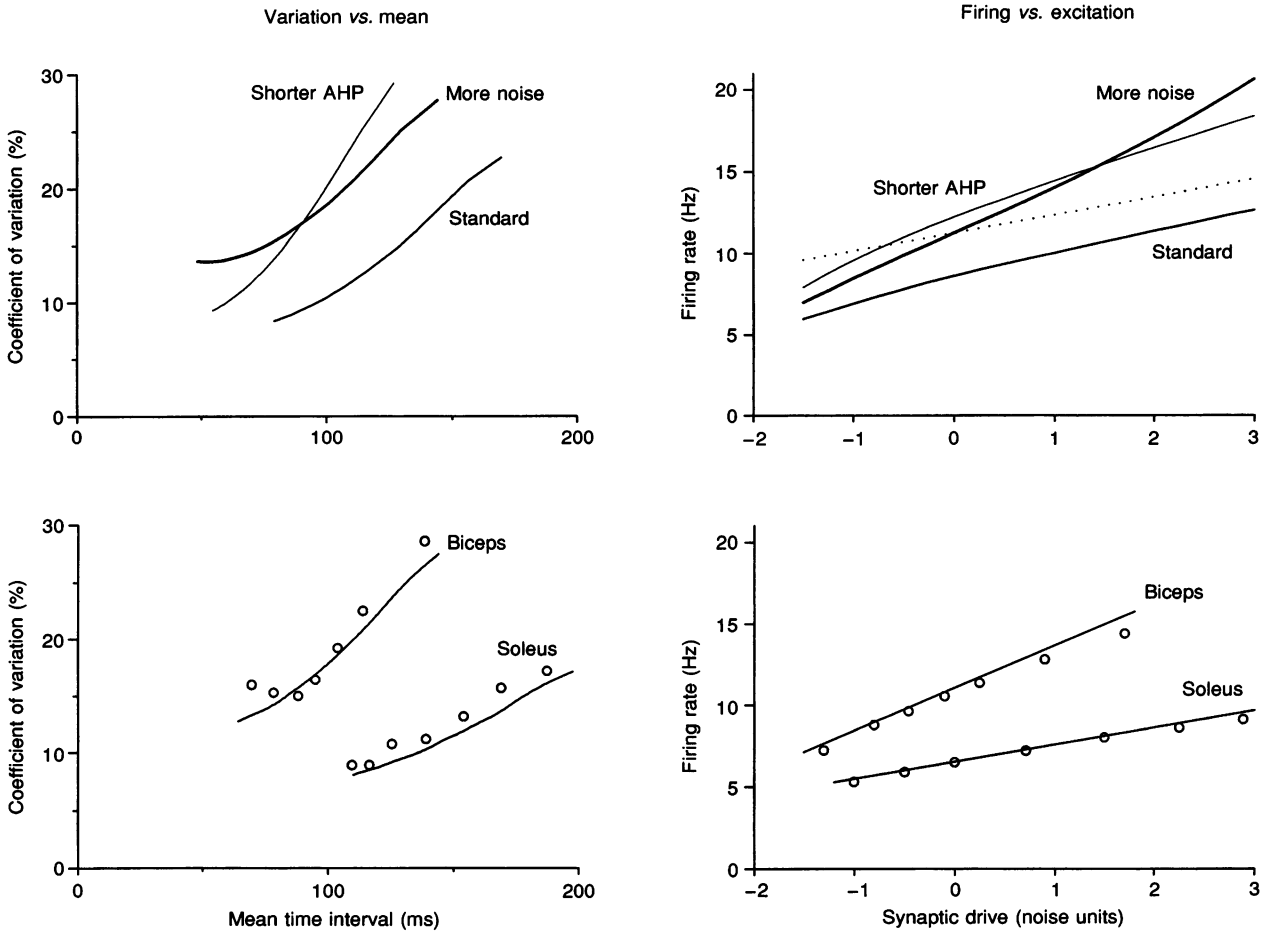

Figure 12. Comparison of model with real data

The top graphs show the separate effects of shortening the AHP, and increasing the synaptic noise on the response of the model to varying levels of synaptic drive (duration of AHP reduced by one third, or noise increased 2·5 times). The curves join a series of invisible points obtained from a series of interval histograms like those of Fig. 11. Relative to the standard, both alterations increased the mean firing rate for a particular synaptic drive and also the variability of discharge at any given firing rate, but they differed in their action on the underlying relationships. In the bottom graphs, the points (O) are for the real motor units of Fig. 7 while the curves are from the model, using the AHP values for these particular units; there is reasonable agreement. In the left-hand graphs, the coefficient of variation of the interval histograms is plotted against their mean. In the right-hand graphs, the mean firing rate (reciprocal of mean interval) is plotted against the amount of synaptic drive. The drive is measured in noise units (the S.D. of noise in millivolts, assumed unaffected by the change in drive); zero is the drive that brings the final equilibrium of the trajectory to threshold. The value of the noise unit, measured in millivolts, will be greater for the more noise plot; the dotted line in the top right-hand graph shows the effect of rescaling its drive in terms of the noise units of the standard, thereby making the absolute units of the abscissa the same for all 3 plots. (In the top graphs the values for the AHPs were: time constants, 30 and 20 ms; initial amplitudes, 50 and 20 noise units; the absolute size of the AHP in millivolts may be assumed constant, so reducing its amplitude in noise units corresponds to increasing the noise level. For comparison, the time constants were 29 ms for biceps and 41 ms for soleus; the initial amplitudes of their AHPs were 24 and 50 noise units, respectively.)

experimental data for each histogram (cf. Figs 1 and 6), and a few unduly long intervals have a disproportionate effect on the coefficient of variation. In accordance with this view, the agreement between the variability plots was considerably improved by removing the last 4% of long intervals from both the real and the synthetic histograms. The mean difference between the coefficients of variation for these eleven units was then reduced to 1·7 ± 1·1% (means ± S.D.); put another way, the 'filtering' reduced the mean of the experimentally observed coefficients of variation by over twice as much as those of the model (by 3·4 *vs.* 1·4%).

DISCUSSION

The present analysis shows that noise plays a major role in excitation during tonic firing of human motoneurones. Thus the tonic firing produced by intracellular current injection in the anaesthetized cat provides only a partial model of the real-life situation; the excitatory drive is then noise free and the post-spike voltage trajectory of the neurone continues to rise until it reaches threshold and a spike is initiated. In decerebrate and lightly anaesthetized cats, however, the background synaptic noise introduces some variability into the current-evoked discharge; moreover, the observed interval histograms with their slight departures from a Gaussian distribution can be explained in terms of the noise parameters (Calvin & Stevens, 1968). The present effects in man are much larger, especially for low firing rates. This is to be expected, since the tonic firing is entirely due to synaptic drive with its inherent noisiness (in the cat data, the coefficient of variation was only 5%, contrasting with the present 10–30%, as in other human recordings). During low-frequency firing, a third of the spikes may occur after the motoneurone has recovered from the preceding spike and be due solely to the noise, being triggered while the mean value of the membrane potential is nearly static and well below threshold. The deviation from threshold often exceeded the standard deviation of the noise, which was probably 1·5–2 mV (see later). Such noisiness is of interest for a variety of reasons, which will be considered after examining the validity of the analysis.

Assessment of analytical methods and modelling

The present raw material is commonplace, consisting simply of interval histograms whose shape varied with mean frequency in a way that has long been familiar. Two special features of the histograms facilitated their detailed study. First, by virtue of using surface recording they contained an unusually large number of intervals. Second, they were based upon relatively homogenous samples of spikes obtained when the running mean frequency of firing fell within certain chosen limits. The novelty lies in the analysis, especially in the use of a transform to deduce the trajectory voltage, necessitating a careful scrutiny of its underlying assumptions and simplifications. The initial stages of data transformation are simply algebraical, without involving modelling with its attendant uncertainties. They provide direct qualitative backing for many of the present conclusions. The modelling was needed to provide quantitative estimates. The broad picture is thus considered secure, although the numerical details cannot be taken as exact. The starting point was the demonstration that an asymmetrical histogram, often simply described as a skewed Gaussian curve, has a tail which proves to be closely exponential once sufficient spikes are collected to smooth out the statistical irregularities. This observation owes nothing to modelling and suffices to show that following a spike, the motoneurone membrane potential comes to equilibrium appreciably below threshold when it is firing at low frequency; but modelling is required to estimate the magnitude of the deviation of the equilibrium potential from threshold, with important implications (see later). The next feature of the analysis was the algebraical transformation of an ordinary interval histogram into an interval death rate plot, giving the conditional probability of the motoneurone discharging a spike in the next unit of time at each time following a preceding spike. The exponential tail of the histogram gives a constant death rate, corresponding to the probability that noise will trigger a spike when the mean potential is at equilibrium but below threshold.

The modelling was then introduced in order to estimate the underlying relation between this probability and membrane potential, thereby enabling the death rate plot to be transformed into an estimate of the trajectory of membrane voltage; this was scaled in units of the noise standard deviation and the firing threshold was taken as zero. The model employed physiologically appropriate values for the noise and its behaviour did not change greatly when these were varied; the temporal correlations within the noise played a crucial part in determining its behaviour, in agreement with theory (Kirkwood & Sears, 1991). Next, the last part of the AHP was determined by combining a number of separate trajectories for different firing frequencies, involving yet further assumptions; the validity of obtaining the different frequencies by slicing has been considered in Results. Finally, the AHP was fitted with an exponential, and the parameters of this curve fed back into the model to produce synthetic interval histograms. The later transformations gain their justification partly empirically, by providing consistent results between motoneurones, and, more significantly, by being based on known motoneurone properties that are formalized in the simplified model. The final validation is provided by the ability of the modelling to predict the relation between firing variability and mean interval for individual motoneurones from their estimated AHP (Fig. 12); direct measurements of variability played no part in determining the two parameters of the AHP (amplitude and time constant). Given its simplicity, the present model does surprisingly well in making intuitive sense of the rich variety of histograms found for a variety of motoneurones firing at a variety of frequencies. The model was deliberately kept simple and incorporated a number of assumptions which cannot be strictly true. However, some of the potential

errors appear to cancel out, so that the final estimates of AHP may not be too greatly in error. In principle, this could be checked in animals by recording intracellularly from motoneurones while exciting them tonically by reflex action. It would then also be worth expanding the model. Many of the present simplifications could be circumvented by starting with the underlying conductance changes rather than dealing solely in terms of membrane potential (Kernell, 1968; Jack, Noble & Tsien, 1983), and confirmatory results have been obtained in this way in preliminary experiments with M. D. Binder and R. K. Powers of University of Seattle, WA, USA. However, the difficulty remains that the choice of values is inevitably somewhat arbitrary, given that the real neurones will be receiving a mixture of excitation and inhibition. The present simplifications are reviewed in the Appendix, with the conclusion that the deficiencies of the model are unlikely to have invalidated the whole approach. Estimates of the equilibrium level of the trajectory are more liable to error than those of the duration of the AHP.

Shape of the AHP trajectory

Present observations. The present analysis suggests that over the final part of the interspike interval, the membrane voltage trajectory is fairly closely exponential. This agrees with the biophysical evidence that the last part of the AHP is due to a change in potassium conductance which decays exponentially with time and is voltage independent (Kernell, 1968; Baldissera & Gustafsson, 1974*a*; Baldissera, Gustafsson & Parmiggiani, 1978; Schwindt & Crill, 1982). The AHP voltage cannot then be strictly exponential, since it does not precisely mirror the conductance, but for small changes near threshold the deviation should be small. The time constants of the present estimated AHPs fall within the range expected from the direct recordings of the AHP of a variety of motoneurones made by Eccles, Eccles & Lundberg (1958). They gave values for the total duration of the AHP rather than its time constant, and these ranged from 60 to 180 ms; in their recordings, the AHP appeared to be prematurely terminated by a delayed negative after-potential. On Kernell's (1968) dictum that the time constant equals a quarter of the duration, the present values of time constant (20–40 ms) correspond to durations of 80–160 ms. The present values for soleus muscle were at the top end of the range, as in the recordings. Direct measurements by Baldissera *et al.* (1978) on four particular motoneurones gave time constants of 13–26 ms for the underlying conductance change. The present values do not go as low as the direct values, probably because the recording discriminated against large, high-threshold units with short AHPs.

An unsettled detail is whether the tail of the AHP during voluntary action is exponential to the very end or whether it is terminated slightly prematurely by some other process, as suggested for the cat (Eccles *et al.* 1958). The cell membrane contains voltage-activated channels that respond with an appreciable delay (Schwindt & Crill, 1982), and which might become important as the 'pure AHP' conductance tends to zero. The present findings are equivocal. Quite commonly, the exponential creep was cut short, but this was probably mostly due to a failure of the slicing to isolate sufficiently pure subpopulations of spikes for a given firing frequency (cf. Fig. 6). On other occasions, the exponential creep continued to the limit of accurate measurement. This uncertainty was bypassed by neglecting the final tail of the 'observed' AHP trajectory when fitting it with an exponential; thus it did not vitiate the comparisons between motoneurones.

Comparison with trajectories recorded during current injection. At first sight, the present trajectories for tonic firing elicited by synaptic drive conflict with those directly recorded from motoneurones excited by current injected intracellularly (Schwindt & Calvin, 1972, 1973; Baldissera & Gustafsson, 1974*a*), quite apart from the differences in scaling (noise units *vs.* millivolts) and reference level (spike threshold *vs.* zero millivolts). However, the differences are readily explained and highlight the limitations of the intracellular work in providing a model of the human situation.

The lowest firing rates are not easily studied with injected current and tend to be avoided; maintenance of a consistent firing rate makes great demands on the stability of the motoneurone. Moreover, any residual noise distorts the trajectory that it is desired to measure, obscuring its true form. The human trajectories, derived from the interval distribution, are a statistical average of the underlying AHP rather than a description of the actual voltage trajectory leading up to any particular spike. A high level of synaptic noise does not prevent the statistical demonstration of the AHP, while obscuring it for the individual case. Thus, the present AHPs with a long tail would not be commonly observed with current injection, and if seen might be taken as trivial examples of isolated AHPs; they are, however, found on modelling the motoneurone (Baldissera & Gustafsson, 1974*b*).

At slightly higher firing rates, at the very bottom of the primary range with injected current, the trajectories obtained by the two methods are in reasonable accord. The recorded trajectories then consist of an approximately constant 'scoop' followed by a linear ramp; the slope of the ramp increases with the current and thus with the frequency of firing (Schwindt & Calvin, 1972). Ignoring any tail, the present trajectories for comparable firing rates are also approximately linear, with their slope increasing with frequency. The matching between trajectories with different algebraical formulations is facilitated by the need to perform it over only a small part of the interspike interval. For any particular frequency, the present method provides only a short segment of the trajectory; with increasing frequency, this spans a progressively earlier part of the exponential AHP, so its slope increases (Fig. 7). For the bottom of the primary range the present model is basically the same as that used by Calvin & Stevens (1986), which was tested numerically in the cat.

At moderate to high firing rates, probably well beyond those currently studied, the recorded trajectories show

changes in the depth of the scoop as the current is increased, typically without a change in the slope of the ramp (Schwindt & Calvin, 1972; Schwindt & Crill, 1982); possibly, the ramp is actually slightly curved (Baldissera & Gustafsson, 1974*b*). This is all quite different from the present observations. It would be interesting to extend the present analysis to high firing rates, when several types of channel contribute to the conductance change at the time of firing, successive AHPs summate, and the spike threshold rises.

Voltage, current and conductance. It must next be emphasized that when determined over a wide frequency range by compounding the effects of various levels of synaptic drive (Fig. 8), the present computed trajectories should differ consistently from the voltage trajectories recorded intracellularly. The reason is fundamental, and is that the present compound trajectory should correspond more closely to the time course of the conductance generating the AHP rather than to the actual voltage trajectory recorded within a given interspike interval. The present trajectories should correspond to the voltage trajectory that would be obtained if the equilibrium potential for the AHP lay far away, whereas the beginning of the real voltage trajectory may approach this value and so be attenuated. However, the various individual short trajectories, each determined for a single level of synaptic drive, all relate to the same level of membrane voltage, namely close to threshold (i.e. within 2·6 noise units, probably below 5 mV, see later); the conductance and voltage trajectories should then be virtually interchangeable as explained below (see eqns (11.11)–(11.13) in Jack, Noble & Tsien, 1983). At the end of the AHP, its underlying conductance will be small in relation to the sum of the other membrane conductances. To a first approximation, the slope of the voltage trajectory will then be linearly related to that of the conductance trajectory so that the shape of any individual trajectory is the same for both voltage and conductance. The increase in slope of trajectories for higher firing rates simply reflects the fact that the AHP is being probed earlier in its time course, when both the conductance and its rate of change increase. Intracellular recordings for low firing rates commonly show such a progressive increase of slope of the voltage trajectory when it is measured at a fixed DC potential near threshold, so there is no major conflict with experiment.

The present compound trajectory was produced by shifting the individual trajectories vertically so as to superimpose their regions of overlap (Fig. 8). Viewed as a conductance, such vertical shift is in order, since AHP conductance is unaffected by voltage (Baldissera & Gustafsson, 1974*a*). On viewing the trajectory as a plot of the voltage of the AHP, this corresponds to the assumption that, for the range studied, the membrane potential is sufficiently far from the potassium equilibrium potential for the current generated by a given AHP conductance to remain nearly constant. This is reasonable when the trajectory is within a few millivolts of threshold, since the potassium equilibrium potential is probably some 20–30 mV below threshold (Baldissera *et al.* 1978). It also assumes that the change in conductance produced by the increase in synaptic drive is a small proportion of the total membrane conductance (otherwise a given change in AHP conductance would produce a smaller change in potential, possibly offset by a change in the size of a noise unit, as discussed in the Appendix). These two assumptions correspond to treating the synaptic drive as the injection of a constant current. The amount of shift of each individual short trajectory required to place it on the compound curve then represents the voltage shift produced by the synaptic current. Significant correction would probably be required to the initial part of the present AHPs to convert them reliably to voltage, since they commonly started 4–5 noise units from threshold (probably corresponding to about 10 mV). Even viewed as conductances, they must be slightly in error because of the various simplifying assumptions.

When comparing the present trajectories with published voltage trajectories it should be noted that the latter have often been superimposed by shifting them horizontally as well as vertically so that they match at the moment of spike generation, whatever the firing rate. While pictorially effective, this is quite different in functional terms. There is then no general relation between the AHP conductance (or resultant current) and the voltage for the family of normalized trajectories, since a given time (measured backwards from the moment of spike initiation) corresponds to very different stages of the AHP (measured forwards from the preceding spike).

Absolute amount of noise

In conjunction with published illustrations for intracellular current injection, the present data permit an estimate of the absolute amount of synaptic noise, in millivolts, in human motoneurones during voluntary activation. This may be done by comparing the present trajectories, scaled in noise units, with those recorded in the cat and scaled in millivolts; these are both extrapolated back to time zero (the preceding spike) and the values equated. A number of assumptions are involved and so the resulting values are very approximate, but they are in line with direct recordings of noise in cat motoneurones.

Assumptions. The first requirement is to decide upon a value for the size of the directly recorded AHP at time zero. A value of 10 mV is often used (Nordstrom *et al.* 1992; Warren *et al.* 1993), but this seems unduly low. The total excursion of the trajectory, from the bottom of the scoop to the firing level at the top of the ramp, is often 12 mV or more during low-frequency firing (Calvin & Stevens, 1968; Schwindt & Calvin, 1973; Schwindt & Crill, 1982); this provides the basis for comparison with the present data, rather than the smaller values seen with higher-frequency firing. Moreover, the scoop takes some 20 ms to develop its

maximum size and so underestimates the time zero value. Extrapolating the trajectory back to time zero gives a value of about 15 mV, which is probably still an underestimate.

The serious problem is to decide how to extrapolate the present trajectories back to time zero. The computed trajectories were exponential. Nonetheless, a linear extrapolation was performed from the approximately linear segment spanning the vertical range 1–2 noise units from the final equilibrium (occupying less than a quarter of the duration of the AHP). This was done because the present trajectories are essentially conductance trajectories (see above), while they are being compared with genuine voltage trajectories. When the membrane potential is close to threshold at the end of the interspike interval, the two types of trajectory will have very similar shapes, and can be interconverted with a constant scaling factor; thus comparison is justifiable. Using an exponential to extrapolate the present curves back to time zero should give an appropriate value for the conductance, but a quite inappropriate value for the voltage, because a given conductance produces progressively less voltage change as its equilibrium potential is approached. The essential assumption is that over the chosen segment, the computed trajectory corresponds sufficiently closely to a voltage trajectory to permit it to be extrapolated back to time zero to give the size of the AHP in units of voltage, albeit scaled in noise units (the S.D. of noise voltage).

The segment spanning 1–2 noise units was chosen for the linear extrapolation because it was both sufficiently short for a linear approximation, and reasonably clear of the final curvature with its potential inaccuracies (cf. Fig. 8). Published trajectories for current injection do not include the final tail of the AHP, so it would be inappropriate to use the slope of this portion of present AHPs for extrapolation. However, varying the precise segment used for extrapolation had rather little effect on its slope. The zero of the AHP was taken as the final plateau of the trajectory; this corresponds to the trajectory coming to equilibrium at threshold.

In a sample of twenty motor units with typical trajectories, the linear extrapolation at time zero fell in the range from 7 to 10 noise units. Equating this with the 15 mV obtained by intracellular recording makes the standard deviation of the synaptic noise 1·5–2·2 mV. Two further motoneurones, both supplying intrinsic hand muscle, had higher than normal noise levels, with standard deviations of just over 3 mV. It was notable that similar values were obtained for motoneurones whose AHPs differed very greatly in duration, falling in different regions of voltage–time plots like those of Fig. 9. This is another facet of the observation that, treated as exponentials, the various AHPs differed chiefly in their time constants rather than their initial values. However, because the time constant may sometimes have been slightly in error, the present linear extrapolation should provide a better measure of the relative amount of noise for the different units. These estimates of the absolute noise show that for low firing rates, the voltage trajectory stabilizes itself about 2 mV below threshold, leaving the noise fluctuations to determine the moment of excitation.

The peak-to-peak noise may be taken to extend to two standard deviations either side of the mean (95% limits for normal distribution) to provide a figure for comparison with recordings in the cat. The present values were 6–9 mV. Granit, Kellerth & Williams (1964) show values around 4 mV during muscle stretch; their cats were always lightly anaesthetized, even when decerebrate. Gustafsson & McCrea (1984) give values of 1·5–3·5 mV during maximal muscle stretch in anaesthetized cats. Calvin & Stevens (1968), using some anaesthetized and some decerebrate cats, stated that the noise was 'usually of the order of 2 mV peak-to-peak, but in some cells it reached a peak-to-peak amplitude of 8 mV'. They also noted that Nembutal anaesthesia greatly reduced the noise; in their example, a supplementary dose of half the anaesthetic dose reduced the noise standard deviation from 2·8 to 1·5 mV (i.e. from 11 to 6 mV peak-to-peak). The present estimates of the synaptic noise in unanaesthetized human motoneurones are thus entirely in line with the limited direct recording.

Noise and trajectory shape: implications for methodology of human studies

The present findings have an immediate relevance to various measures of motor unit activation, since the detailed interpretation of all such measures is inevitably based on a model of the motoneurone and its excitation. This has previously led to much debate. The importance of synaptic noise is widely recognized in both theory and practice; a well-studied example is that noise affects the relation between the shape of the post-stimulus time histogram (PSTH) of a motor unit and the waveform of a brief depolarization of the motoneurone, such as an EPSP (Kirkwood, 1979; Gustafsson & McRea, 1984; Midroni & Ashby, 1989; Kirkwood & Sears, 1991; Kenyon, Puff & Fetz, 1992). The present findings show that noise is an inescapable, major contributor to low-frequency tonic firing. As a corollary, any analysis which ignores its action is suspect; most human studies deliberately employ low firing rates, and even high firing rates will be affected. The noiseless motoneurone is an inadequate model for studying excitation in man.

The models underlying the analysis of human data usually incorporate assumptions about the trajectory of the motoneurone, with everything treated in terms of voltage rather than conductance, even for the first part of the AHP. The trajectory is typically taken to be a linear ramp starting at a fixed value of scoop, with excitation occurring simply when the ramp reaches threshold (for example, Ashby & Zilm, 1982; Fetz & Gustafsson, 1983; Nordstrom *et al.* 1992; Warren *et al.* 1993). Noise has often been entirely ignored, in spite of its recognized theoretical importance (Kirkwood & Sears, 1991). Most authors assume that the slope of the linear ramp increases with the firing frequency, while usually recognizing the conflict with typical intracellular recordings (variable depth of scoop, fixed slope of ramp). The variable slope model is justified by the observation that on varying the mean firing rate, a testing EPSP still produces much the same effect (expressed as the

percentage of spikes in PSTH), which is incompatible with a constant ramp slope. At moderate firing rates, the present exponential trajectories would give the same result, since a short segment of an exponential approximates to a straight line with its slope increasing with the firing rate (see Fig. 7). At low firing rates, however, the constant slope model may fail, and the trajectory has recently been suggested as having a final slower approach to threshold in accordance with some earlier modelling (Baldissera & Gustafsson, 1974*a*, *b*; Piotrkiewicz, Churikova & Person, 1992; Olivier, Bawa & Lemon, 1995). Ashby & Zilm (1982) noted that 'exponential rather than linear trajectories would ... modify the behaviour of the model ... in a complex but essentially predictable manner'. The linear model would appear to have been chosen for its simplicity, but the details of its behaviour cannot be trusted, especially for low firing rates. Three types of analysis merit comment in the light of the present evidence that the trajectory is exponential and that synaptic noise crucially determines excitation.

(1) PSTH

As is well recognized, the conventional peri-stimulus time histogram is a complex affair with no simple general relation between the shape of the EPSP and the form of the resulting PSTH. The present experiments contribute by showing that the PSTH typically contains spikes evoked during totally different phases of the trajectory, namely both during its rapid phase, when it is an approximate ramp, and its final exponential tail, when noise is dominant. The relation between the EPSP and the PSTH probably differs for these two situations, perhaps with the shape of the PSTH shifting further away from the first differential of the EPSP towards its direct representation. If so, the particular mean firing rate chosen for study will be important since it will determine how much of the overall PSTH is derived from the rising phase of the trajectory and how much from its nearly horizontal tail.

The difficulties of interpretation are reduced but not entirely eliminated on refining the situation and triggering the stimulus from a spike, and so repeatedly testing 'excitability' at the same point on the trajectory (usually before any spikes occur normally). In the absence of noise, the motoneurone would respond the same way every time, either firing or not firing. In the presence of noise, the unit will alternate between responding and not responding, and its probability of firing will be a function of the size of the EPSP, the distance of the trajectory from threshold and the amount of noise (also the time structure of the noise and of the EPSP). The situation thus invites the present type of analysis, which is potentially capable of improving upon the PSTH, especially for long testing intervals with spontaneous spikes, as when studying recurrent inhibition (Meunier, Pierrot-Deseilligny & Simonetta-Moreau, 1994). The underlying relation between voltage and probability can be expected to be Gaussian rather than linear, so that doubling the underlying depolarization would more than double the 'response', measured as the mean number of spikes evoked in a PSTH. Likewise, when two EPSPs are precisely synchronized, their joint action would exceed their arithmetical sum, thereby mimicking neural facilitation as already shown by others (Kirkwood & Sears, 1991; Kenyon *et al.* 1992).

It follows that the normal PSTH, for random stimulation, is yet harder to interpret in quantitative terms. It will summate all the probabilities for the spike-locked stimulation and will show a peak at the time of the EPSP which increases monotonically with the size of the EPSP; the underlying relation will, however, be complex and is likely to vary with the firing rate of the unit. Measurements of excitability obtained by adjusting the strength of a testing monosynaptic stimulus so as to excite a unit to fire on 50% of occasions will also depend upon a unit's firing rate, even if combined with spike-triggered stimulation. Yet further uncertainties apply to various grosser measures that essentially utilize the surface EMG to compound the PSTH of a number of units, such as averages of the EMG following the discharge of a cortical neurone or following a cortical stimulus, and indeed the simple H reflex itself. Thus, the stochastic properties of the motor unit complicate the development of quantitative measures of synaptic input.

(2) Instantaneous firing frequency

Detailed measurements of instantaneous frequency (the reciprocal of the interspike interval) have recently been combined with spike-triggered stimulation and have been suggested as providing important information unobtainable from the PSTH (Miles, Türker & Le, 1989; Awiszus, Feistner & Schäfer, 1991; Poliakov, Miles & Nordstrom, 1994). In a noise-free model motoneurone with a linear trajectory, such analysis can provide a precise estimate of the shape of the rising phase of an underlying EPSP with far fewer trials than a PTSH (Miles *et al.* 1989). The details of such estimates must now be at risk, since the present, more realistic, model might behave slightly differently.

More seriously, during low-frequency firing, measurements of instantaneous frequency can be grossly misleading when applied to a synaptic input of appreciable duration, such as a stretch response with both short- and long-latency components. For example, when two successive excitatory inputs are actually equal, the second might be taken to be the larger for the following reasons. On delivering the paired inputs repeatedly, at random times, the first input will affect the motoneurone at all phases of its trajectory and will terminate many intervals which are already long, and which would otherwise have contributed to the tail of the histogram; the mean frequency of the spikes that it elicits will thus be relatively low. In contrast, the second input will tend to act on the motoneurone relatively early in its trajectory, since many long intervals will have been terminated prematurely by the first stimulus; thus the relatively few impulses it elicits will have a higher mean

frequency than the more numerous impulses elicited by the first input. Similar considerations apply when inhibition is also introduced. Thus, measurement of mean instantaneous frequency and its derivatives can never provide a reliable index of the level of excitation; the maximum instantaneous frequency achieved would seem more significant, and further statistical measures of frequency and/or interval might well improve upon the PSTH.

(3) Cross-correlogram peaks

General considerations. Short-term synchronization of a pair of motoneurones, occurring over 5–10 ms, seems largely due to their being excited by branches of the same stem fibres. Considerable effort by a number of workers has been devoted to methods of estimating the strength of the common input from an observed correlogram and to allowing for synaptic noise (see Kirkwood & Sears, 1991). The present observations sharpen the perspective by showing that spike initiation is largely dependent upon synaptic noise rather than on the trajectory itself reaching threshold. Moreover, during low-frequency firing many spikes occur when the trajectory is almost flat and well below threshold. This must increase the probability that a given stem fibre will excite both neurones of a pair, since the proportion of time that both neurones are available to be excited by the fibre will be greater than if the trajectory were rising linearly throughout. The increased synchronization of γ-motoneurones that occurs as the firing rate falls has already been explained in essentially the same way (Ellaway & Murthy, 1985).

Theoretical analysis shows that when the trajectory is more than one noise standard deviation from threshold, the synaptic efficacy of an EPSP in triggering firing increases very rapidly with its size (Kenyon *et al.* 1992). The present analysis shows that at low firing rates, the trajectory never rises much above this level. Short-term synchronization should thus be particularly dependent on presynaptic fibres which produce large EPSPs, with their effects 'amplified' by such non-linear behaviour; corticomotoneuronal inputs might well be favoured in this way with their suggested major contribution to short-term synchrony and the related increases in coherence (Farmer, Bremner, Halliday, Rosenberg & Stephens, 1993). However, the motoneurones should also 'be especially sensitive to the synchronous arrival of many EPSPs' (Kenyon *et al.* 1992). Thus any tightly synchronized activity in the population of presynaptic fibres would also be amplified and helped to produce a peak in the cross-correlogram, independent of the extent to which the motoneurones were supplied by the same stem fibres.

Indices of synchronization and modelling. There are a number of ways in which an index of synchronization can be determined, but for a given pair of motor units the value of all the usual indices increases when the firing rate decreases (Nordstrom *et al.* 1992). This limits their utility as a direct measure of connectivity. Nordstrom *et al.* held that the inconstancy occurred for purely mathematical reasons and that their own new index should be unaffected, but the whole issue is clouded by the failure of their eqn (2) to address the realities of the situation (as shown to me by Professor J. R. Rosenberg of Glasgow University, UK). The value of such indices is also positively correlated with the variability of the unitary discharges (Nordstrom *et al.* 1992); synchrony between pairs of γ-motoneurones in the cat also increases with variability (Davey & Ellaway, 1988). The correlation might simply reflect differences in synaptic noise in the various cases, since this should influence both variability and short-term synchronization (Kirkwood & Sears, 1991). As an alternative, it might arise from differences in the intrinsic properties of the motoneurones themselves; the duration of the AHP then emerges as an important variable, with its gross effect on the variability of discharge for a given mean rate (see Fig. 12). Thus, when studying short-term synchrony, it would be interesting to estimate the AHPs of the motoneurones involved from the interval distributions used for making the cross-correlograms.

Wider considerations

The present analysis shows that the varied shapes of the interval histograms found during voluntary activation of single motor units conform to a simple pattern, determined by the interplay between time-filtered Gaussian noise and the AHP. However, the recording techniques selected units with a low threshold, recruited at low forces, firing in the lower part of their frequency range. Although there is no direct information as to what happens beyond these limits, the experiments validated a model whose behaviour may be extrapolated. High-threshold units supplying fast muscle fibres would have shorter AHPs than low-threshold units, so should give a similar range of histograms on a compressed time scale. A unit firing at the top of its frequency range should give an approximately normal distribution, like those in Fig. 11. But there is no substitute for further experiment. It would be particularly interesting to compare the behaviour of motor units within the same muscle with different firing patterns (fast units tend to fire at a higher frequency than slow ones), and to study muscles whose units show little tendency to increase their firing rate with increasing voluntary drive.

The properties of the synaptic drive will be as important as those of the motoneurone in determining the shape of the histogram for a given mean firing rate (cf. Fig. 12); the noise may well differ for a given mean depolarization, when evoked by different types of input. The size of the unitary EPSPs will matter, as will the number of active afferents converging on a given motoneurone. Such change in the synaptic input is held to be responsible for the gross increase in the variability of single γ-motoneurones that is seen when a decerebrate animal is spinalized (Ellaway, 1972). Perhaps the very nature of the synaptic drive is involved, as excitation of α-motoneurones might involve

voltage-sensitive ligand-gated channels as well as voltage-insensitive ones. It would be interesting to study the same motor unit during the performance of different tasks. Not only might the noise vary, but the duration of the AHP itself seems to be under central control; it is much reduced during fictive locomotion (Brownstone, Jordan, Kriellars, Noga & Schefchyk, 1992).

In conclusion, the present type of analysis offers a novel way of studying the descending control of the motoneurone in man, which can be readily performed on both healthy and diseased subjects. It should also be applicable to animal recordings from other types of tonically firing neurones, raising other types of issue; for example, a neurone 'waiting' slightly below threshold could provide a sensitive coincidence detector of synchronized inputs. However, the wider the range of conditions studied, the more important it will become to extend the modelling and incorporate more of the complexities of synaptic activation.

APPENDIX

Modelling the excitation of the motoneurone by noise

Statistical fluctuations in the synaptic bombardment of a motoneurone produce appreciable synaptic noise, so that its membrane potential fluctuates about an otherwise steady level. Intracellular recording shows that such noise may have a peak-to-peak amplitude of several millivolts (Granit *et al.* 1964; Gustafsson & McCrea, 1984) and that it can be formally described as exponentially time-filtered Gaussian noise (Calvin & Stevens, 1968). The extreme fluctuations would be expected to trigger the occasional spike even when the mean depolarization is well below threshold. As the membrane potential approaches threshold, the frequency of noise-induced spikes will increase. Such noise excitation is suggested as being responsible for the exponential tails of the present interval histograms for low firing rates. The relation between the membrane depolarization and the probability of a spike being triggered by noise was thus determined by computer modelling. This was done under static conditions using a motoneurone without AHP, with its membrane potential set to a series of constant values. The resulting transforms were then used to model the behaviour of motoneurones with an AHP and applied to the last part of the trajectory, when the voltage is changing relatively slowly.

The starting point was Gaussian noise, rather than individual synaptic potentials; given the correct time smoothing this is quite in order, since the amplitude distribution of the sum of a large number of separate events is Gaussian (the central limit theorem). This was recognized by Calvin & Stevens (1968) and has been confirmed by computer modelling (Kirkwood & Sears, 1991, their Fig. 10.4 legend). The simplest possible model was used with the aim of bringing out the essentials, rather than achieving final numerical accuracy. All signals were treated as voltages, remaining constant at different mean levels of membrane potential, and the underlying conductance changes were ignored. This should produce relatively little error for small deviations near threshold (see Discussion); this has been confirmed in preliminary studies with a more elaborate model in collaboration with M. D. Binder and R. K. Powers (unpublished).

The novelty in the present modelling is its use to determine the transforms of Fig. 13, rather than simply to produce interval histograms. The forward voltage–probability transform provides a minor convenience as it enables interval histograms to be synthesized more rapidly than by direct simulation. The backward probability–voltage transform opens up quite new possibilities, since it can be applied to real interval histograms to estimate the underlying trajectory. The initial simulations, however, follow a well-trodden path. Calvin & Stevens pioneered such modelling of the motoneurone with a noisy input in 1968, and D. L. Tuck introduced a related model in 1977, which continues to be used (Kirkwood, 1979; Kirkwood & Sears, 1991). Geisler & Goldberg (1966) applied a similar model to superior olivary neurones and certain studies on the well-known leaky integrator model are closely related (reviewed by Jack *et al.* 1983). The concentration on the role of noise is the essential, since this was neglected in much earlier modelling of the response of motoneurones to injected current. There is also an extensive mathematical literature on the determination of 'level crossings' in noisy systems; in a review, Cox & Isham (1980) noted that each individual case has to be considered on its own. Longuet-Higgins (1962) had already emphasized the intractability of the general problem to direct analytical methods, and tested the validity of various approximate solutions numerically using an early computer simulation. Computer simulation was also rapidly adopted by physiologists studying excitation (cf. Gerstein & Mandelbrot, 1964).

General description of the model and its behaviour

Since the amplitude distribution of the noise is approximately Gaussian, it might be thought that when the mean depolarization of a motoneurone is known, then the probability of its being excited by noise in the next millisecond could be directly obtained from standard statistical tables. But this would neglect the temporal structure of the noise, which is as crucial as its amplitude distribution; an example is that spikes are only triggered when the threshold is approached from below, not from above. The situation was modelled as follows.

First, 30 000 serial values of Gaussian noise were calculated (zero mean, unit S.D.) corresponding to sampling the membrane potential at 1 ms intervals. The series was then time smoothed to create the temporal correlations; each member of the new series consisted of the exponentially weighted sum of the original value and the ten preceding values, using a time constant of 4 ms as found by Calvin & Stevens (1968). The mean of the new series approximated

to zero, but its standard deviation was 1·58 times larger than that of the original series; this new value was used as the standard noise unit for scaling the membrane potential, since it is that of the simulated smoothed noise in the motoneurone.

The threshold was then set to one of a preselected series of deviations from zero and each successive value of the smoothed noise series tested to see whether threshold had been reached; if so, a spike was scored and the interval since the last spike recorded. When several successive values were above threshold, the start of the interspike interval was timed from the last suprathreshold value. There was no refractory period or AHP, and every spike reset the timing. However, intervals below 11 ms were discarded since the synaptic noise of the model then correlated temporally; these had no counterpart in life since the real spikes arose at widely separated times. This enabled an interval histogram to be constructed for a particular deviation from threshold (bin width, 1 ms). These histograms were simple exponentials, with statistical fluctuations, showing that there was a fixed probability that the noise would reach threshold and terminate the on-going interval in the course of the next millisecond. This interval death rate was calculated bin by bin, as for the real spike trains (see Methods; calculation terminated when the number of survivors fell below fifty). These values were then averaged (with constant weight) to give a mean probability of the noise reaching threshold in the next millisecond. This was repeated on the same run of noise for a number of different thresholds. Five independent segments of noise were analysed in this way and the results combined (probabilities averaged).

Figure 13*A* shows the resulting 'observed' dependence of the probability of firing on the membrane potential; the points were obtained directly from the model. This particular set of data was used to analyse the real interval histograms; however, as discussed below, changes in the numerical details of the modelling alter the precise numerical values without affecting the general outcome (cf. Geisler & Goldberg, 1964). The values also include a small residual statistical variability. Very slightly different values were obtained subsequently when 3 260 000 successive noise intervals were tested rather than 150 000; but the differences were insignificant in the light of the other uncertainties (see below), and no correction was attempted. The curve fitted to the data is derived from a normal distribution, with the probability value for any potential corresponding to the probability of that value being exceeded by chance (i.e. the area under one tail of the distribution). Thus the behaviour of the model was essentially Gaussian, but because of the temporal correlations in the noise the parameters of the curve (mean and S.D.) differed from those of the noise distribution itself. The values for the curve were used in the computation when synthesizing a histogram from a trajectory.

The Gaussian behaviour was demonstrated by treating each probability measurement as the area (integral) of one tail of a normal distribution from X to infinity and using standard tables to calculate the value of X. A straight line was then obtained on plotting X against the corresponding value of V (membrane potential) on linear scales (correlation coefficient = 0·9996, for V in the range $-2{\cdot}1$ to $+0{\cdot}5$, beyond which small deviations began to appear). This also provided the parameters of the Gaussian distribution involved. Due to the time structure of the noise, these differed appreciably from those for the noise distribution itself (mean shifted from 0 to 1·37, S.D. increased by a factor of 1·52, both in noise units). Similar behaviour was obtained when the time course of the filtering was changed from exponential to linear or hyperbolic.

Such Gaussian behaviour is of interest in relation to a theoretical study by H. B. Bostock, only parts of which have been published (Kirkwood, 1979; Kirkwood & Sears, 1991). After simplifying, Bostock's analytically derived equations state that for time-smoothed Gaussian noise the probability of a threshold crossing from below is again a Gaussian function of the mean deviation from threshold, with its standard deviation depending on the rate of change of the noise as well as on its amplitude (both assumed Gaussian). Cox & Isham (1980) give the same result (their eqn (3.67)). These equations, however, cover the situation in which no spikes are discharged and so are not immediately applicable to the present firing model; Kirkwood & Sears (1991) have already noted that 'considerable changes in membrane potential distribution ... occur near threshold when crossing and recrossing of threshold at short intervals is prevented by spike occurrence'; this has equally been recognized by Warren *et al.* (1993).

Figure 13*B* shows the same data with the axes reversed to provide a calibration that allows the membrane potential trajectories of real motoneurones to be computed, point by point, from their interval histograms. The curve fitted to the data is now simply the sum of two exponentials and has no theoretical basis; it was chosen and fitted empirically to provide a convenient formulation for the routine calculation of trajectories (the Gaussian integral is a non-analytic function). The deduction of the trajectory from the interval histogram data is thus based empirically on the way the model responded to noise with a particular structure, rather than purely on theory. The behaviour of the model was not intuitively obvious at the outset; when the mean membrane potential was at threshold, then the probability of a spike being discharged in the next millisecond was only 18%, not 50% as might be casually supposed.

Application of transform to a moving trajectory

The transform of Fig. 13*B* was determined under steady-state conditions, with the noise disturbing the mean membrane potential around a fixed value; but it was then applied to determine the rising phase of the trajectory as well as its final near equilibrium. This presumably introduced some distortion, since the rate of change of membrane potential should matter as well as its absolute value, and the transform would not work with rapid transients; however, for present purposes the resulting error was probably small enough to be neglected because the time constant of the noise was very much shorter than

that of the AHP (4 ms *vs.* 20–40 ms). Bostock's equations (Kirkwood & Sears, 1991) deal with the related case of an EPSP and suggest that for a change of potential to produce a significant effect, both its amplitude and its rate of change must be appreciable in relation to those of the noise; considering the change in the AHP millisecond by millisecond, both these parameters should have been small within the time scale of the noise, allowing the AHP to be treated as a series of steady states.

This was validated by comparing histograms synthesized with the transform of Fig. 13*A* and those determined by a more direct method that allowed for the trajectory being a dynamic event; good agreement was then regularly obtained, as shown in Fig. 14*A*. The direct method followed most previous practice (see earlier) and summed the AHP with the synaptic drive and smoothed noise millisecond by millisecond, until threshold was reached, when the AHP was reset and a spike scored; this simply incorporates an AHP into the simulation used above to determine the present transforms (for comparability, the noise was still smoothed over eleven bins only). The thick line in Fig. 14*A* shows such a directly obtained histogram, based on 17 520 spikes discharged over 34 min of simulated recording time. The small differences from the histogram given by applying the transform to the same trajectory (thin line) must have been partly due to the statistical errors inherent in determining the transform's parameters, as well as to the slightly different dynamics of the two situations; they do not warrant further discussion.

Value of membrane time constant

In physiological terms, the time constant of the smoothing applied to the noise corresponds to the time constant of the membrane of the neurone. This means that there is an inherent limitation to the accuracy of modelling a particular human motoneurone, because its time constant remains unknown. The passive time constant will differ between neurones, and during tonic firing the value will be reduced by an unknown amount by the opening of inhibitory as well as excitatory channels. As is to be expected, the value of the time constant affects the precise shape of the transforms given by the modelling. This is illustrated in Fig. 13, where the dashed lines show the

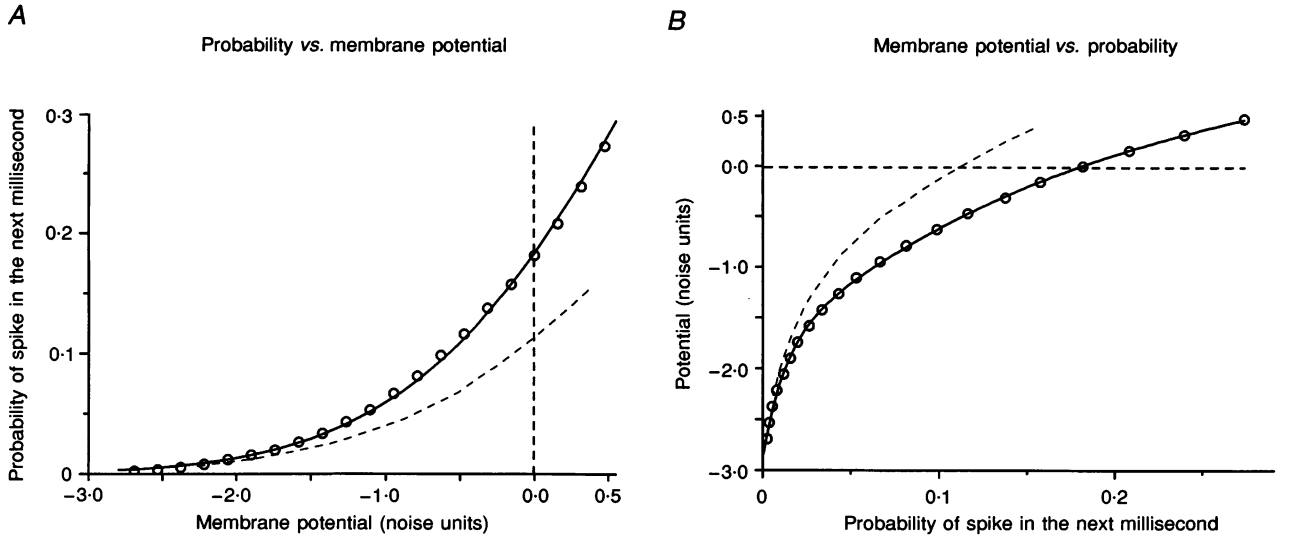

Figure 13. Probability–voltage relations obtained by modelling the effect of noise

Each point was obtained from the model by setting its mean membrane potential to a particular value, adding time-smoothed Gaussian noise, and repeatedly determining the time at which the noise triggered a spike by causing the momentary potential to reach threshold. The probability of its firing a spike during any given millisecond, when it has not yet done so, was calculated for each mean potential, giving graph *A*; the potential is scaled in terms of the S.D. of the noise (1 noise unit), zero is at threshold and negative values represent hyperpolarization. The curve fitted to the points is that for the area under the tail of a Gaussian distribution, but one whose mean and variance differ from those of the noise (see text). *B* shows the same data with the axes interchanged to provide a calibration curve for estimating the membrane potential of real motoneurones from measurements of probability on their interval histograms. The curve fitted to the points is now the sum of two exponentials. It has no theoretical significance, but was convenient for computing trajectories and accurate over the range studied. (Curve parameters: rate constants, 0·0120 and 0·2039 probability units; starting values, −1·054 and −3·096 noise units; equilibrium value, 1·276 noise units.) The membrane time constant of the model was 4 ms, but because of the finite bin width used, the transforms apply to a neurone with a slightly longer time constant (see text). The dashed lines join the (invisible) points obtained when the time constant was doubled (8 ms).

effect of doubling the time constant from 4 to 8 ms (both for 1 ms bins). The deviation from the 4 ms data increases as threshold is approached, and is somewhat less serious around the region of particular present interest, namely 1 noise unit from threshold; for example, if the 4 ms probability–voltage transform is applied to data from an 8 ms motoneurone, it falsely gives the voltage as 1·25 noise units when the correct value is 0·85 noise units (for the same false value, the true value would be 1·0 for a 6 ms neurone, and 1·5 for a 2 ms neurone). The false values are of the right order of magnitude, but sadly lacking in numerical precision.

Figure 14*B* compares the trajectories obtained by applying the 'right' and 'wrong' transforms to an entire interval histogram. The continuous line shows the input trajectory applied to a neurone with a time constant of 8 ms to synthesize an interval histogram (by using the 8 ms voltage–probability transform, histogram not shown). The filled circles show the successful re-creation of the trajectory on applying the 8 ms probability–voltage transform to the histogram. This also helps validate the two transforms as computational tools, by confirming that they are inversely related. On the evidence of Fig. 14*A*, the underlying trajectory would also be recovered effectively on applying the probability–voltage transform to a histogram obtained by conventional time-based simulation.

The wrong trajectory in Fig. 14*B* was obtained by applying the 4 ms transform to the 8 ms histogram. It systematically overestimates the deviation from threshold, but retains much the same general form and remains fairly closely exponential. Fitting these particular points with an exponential gave a time constant that differed by only 4% from the value for the original input trajectory. Compounding several such false trajectories for several synaptic drives, as was done with the real motor unit data (Fig. 8), also gave an approximately exponential trajectory, with its time constant again only differing very slightly from the correct value (difference again 4%, but now the time constant was underestimated rather than overestimated; these small differences are within the error of the estimates, but more probably result from the non-linear relation between the 4 and 8 ms transforms). However, the initial size of the AHP was appreciably underestimated in both cases (by 17 and 7%, respectively). It may be concluded that the use of an inappropriate transform on physiological data can produce appreciable errors in the

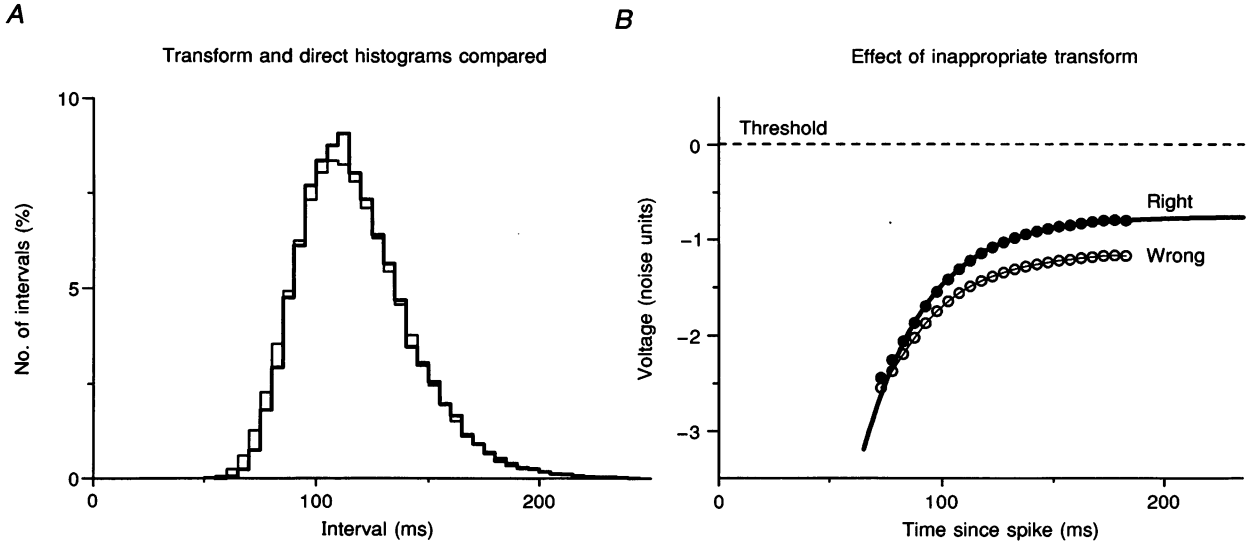

Figure 14. Testing the transforms

A tests the voltage–probability transform of Fig. 13*A*. The thin line shows an interval histogram synthesized using the transform of Fig. 13, as in Fig. 11. The thick line shows the histogram produced by a more direct method (see text) for the same model motoneurone, with the same synaptic drive (−1 noise unit, 4 ms membrane time constant, AHP as in *B*). The 2 histograms have similar means and coefficients of variation (117·4 and 118·2 ms; 22·1 and 21·2%). *B* tests the effect of using a probability–voltage transform derived from a motoneurone with the 'wrong' membrane time constant. The thick curve shows the input trajectory applied to a motoneurone with a time constant of 8 ms to create the histogram for analysis. Applying the 8 ms transform to the histogram gave the 'right' curve (●), which re-created the original trajectory. Using the standard 4 ms transform gave the wrong curve (○). This curve is qualitatively similar, but significantly overestimates the displacement of the trajectory from threshold; the approximate equilibrium potential was shifted from −0·8 to −1·2 noise units. (Synaptic drive, −0·75 noise units; AHP time constant, 28·6 ms; initial size, −23·7 noise units, corresponding to the values for the biceps unit of Fig. 8.)

estimate of the absolute level of the trajectory, while having remarkably little effect on the estimate of the time constant of the underlying AHP.

In the present experiments, the transform for a 4 ms smoothing time constant was applied to all motoneurones; this was the time constant found by Calvin & Stevens (1968) in a motoneurone with appreciable synaptic noise, but leakage around the electrode might have caused it to be slightly low. Many quiescent motoneurones have appreciably longer time constants (Jack, Miller, Porter & Redman, 1971; mean value, 5·8 ms; range, 2–14 ms), but steady synaptic activation should reduce the value. In making comparisons it should be noted that the present simulations introduced some additional smoothing by using the finite bin width of 1 ms, so that the use of the 4 ms transform approximated to the behaviour of a motoneurone with a membrane time constant of 5 ms (see below). The data of Fig. 13 thus provide a reasonable compromise between competing uncertainties, but no one transform can provide numerically exact estimates for all motoneurones; nothing better can be done until the time constant of the individual motoneurone can be estimated. The errors should usually have been rather smaller than those illustrated in Figs 13 and 14.

Effect of bin width. Using a bin width of 1 ms to calculate the transforms inevitably helped smooth the noise, since this was calculated bin by bin. Thus, in accordance with the effect of changing the smoothing time constant, reducing the bin width to 0·5 ms shifted the probability–voltage curve upwards (cf. Fig. 13). The original 4 ms transform corresponded rather closely to the transform for 5 ms smoothing calculated with 0·5 ms bins. However, it is not suitable simply to use a very short bin width, say 0·1 ms, as some such smoothing is physiologically appropriate to allow for the finite rising time of individual post-synaptic potentials which will filter out the highest noise frequencies. For a unitary Ia EPSP, the rise time may vary between 0·2 and 2·8 ms (Jack *et al.* 1971; 10–90% rise times, modal value 0·5 ms, mean approximately 0·7 ms). The effect of introducing a finite rising time to the noise was studied by reducing the bin width to 0·25 ms and introducing a high-cut filter by two-point smoothing of the original random number series, thereby spreading the rise of each of the original noise steps over 2 bins (before the exponential smoothing). The transforms for a filtered 0·25 ms bin width series were then very close to that for an unfiltered 0·5 ms bin width series; without such filtering the smoothing time constant had to be increased to 6 ms to match the original transform of Fig. 13.

Duration of smoothing. The smoothing calculation stopped looking back after 2·5 time constants to ensure that a run of noise which brought the membrane to threshold played no part in the excitation of the next spike contributing to the interval histogram (intervals shorter than this rejected, see earlier). When the smoothing was allowed to run its course, the resulting transform showed very little change (a shift of less than 0·05 noise units in the region of 1 noise unit); this also introduced some inappropriate correlations in the noise, since spike collection still started 2·5 time constants after the last spike (this cannot be delayed indefinitely, as too few valid spikes are then obtained). No major effect would be expected since a noise spike had decayed to 6% of its initial value when it was first ignored. The unimportance of restricting the duration of the smoothing was confirmed on synthesizing interval histograms by the direct method of Fig. 14, which allows the duration of smoothing to be increased to infinity; for the example in Fig. 14, this increased the mean of the histogram by 0·7% and its coefficient of variation by 2·7% of the stated values.

Further assumptions

Several simplifications underlying the modelling deserve emphasis, since they might affect the numerical details of the estimate of the AHP; but they should not compromise the overall conclusions.

(1) Noise structure. The actual structure of the synaptic noise is unknown for man and might vary with the conditions. That used was taken from recordings in the cat, and was a time-smoothed Gaussian distribution. Small changes in the smoothing produced only secondary effects on the model and its transform from probability to voltage. But large EPSPs from large pyramidal tract axons might have a special role to play in voluntary excitation and might perhaps positively skew the noise amplitude distribution, with consequences that remain to be explored.

(2) Spike threshold. The voltage threshold of the neurone was assumed to be constant, whereas in some motoneurones it may be slightly raised following each spike (Calvin & Stevens, 1968; Schwindt & Crill, 1984). This is largely immaterial for the present modelling, which will simply lump any threshold change in with the AHP; it would matter if the computed AHP could be compared with actual intracellular recordings.

(3) AHP summation. The model ignored any summation between successive AHPs, as recorded by Ito & Oshima (1962), with its tendency to produce a negative correlation between successive intervals. This might increase the tail of the interval distribution, and make the computed AHP longer than that following an isolated spike. At the worst, the potential error corresponds to averaging AHPs with amplitudes varying by up to 15%, but with the same time constant. (The shortest intervals corresponded to about twice the AHP time constant, which would make the ensuing AHP 13·5% larger than that following a very long interval; any residual AHP at the time of a spike sums approximately linearly with its successor; Baldissera & Gustafsson, 1974*b*.) In a closely related model, the retention of the residual AHP from one interval to the next made little difference (Geisler & Goldberg, 1966). On extending the present model, this slightly increased the mean of 'direct' histograms like that of Fig. 14*A* while slightly reducing their coefficient of variation (about 1% change for both).

Likewise, the determination of the final third of the full AHP by superimposing the trajectories from the interval distributions for different levels of synaptic drive (producing different firing frequencies) assumes that the AHP does not change with the firing rate. Also, the AHP is assumed to sum linearly with the drive, as widely believed (Kernell, 1968; Schwindt & Calvin, 1973).

(4) Effect of synaptic drive on noise level. It was assumed that the noise amplitude remained constant when the mean synaptic drive changed. This cannot be strictly true, but for the following reasons the changes in noise level were probably small; the estimated AHP would then be slightly distorted without becoming entirely unreliable. First, the percentage increase in the net amount of synaptic drive (mean depolarization) required to produce the present spread of firing rates was probably below 50%, since this is how models with a threshold typically behave (Jack *et al.* 1983). Second, the noise may be expected to increase as the square root of the drive, rather than in direct proportion, since it is produced by the summation of an irregular series of synaptic potentials which should show Gaussian behaviour. A 50% increase in drive should thus correspond to a 22% increase in noise amplitude. Third, the membrane conductance will increase with the level of synaptic drive, thereby decreasing the voltage swing produced by each unitary synaptic event. This, however, is not easily quantified since any concomitant inhibition will act both to decrease the noise voltage by increasing the conductance further, and to increase it by increasing the number of synaptic events for a given net depolarization.

(5) Effect of AHP conductance on noise. The noise amplitude was also assumed to remain the same for the whole of the AHP; again this cannot be strictly true, since the conductance changes throughout its course. Within an individual trajectory the effect should be small, since each spans only a small segment of the full AHP. At low firing rates, dependent on the tail of the AHP, the absolute value of the AHP conductance will be low and it will contribute relatively little to the overall conductance. At high firing rates, however, the AHP conductance probably matters and should reduce the noise level, providing further compensation for the noise increase produced by the greater synaptic drive.

ADRIAN, E. D. & BRONK, D. W. (1929). The discharge of impulses in motor nerve fibres. Part II. The frequency of discharge in reflex and voluntary contraction. *Journal of Physiology* **67**, 119–151.

ASHBY, P. & ZILM, D. (1982). Relationship between EPSP shape and cross-correlation profile explored by computer simulation for studies on human motoneurons. *Experimental Brain Research* **47**, 33–40.

AWISZUS, F., FEISTNER H. & SCHÄFER, S. S. (1991). On a method to detect long-latency excitations and inhibitions of single hand motoneurons in man. *Experimental Brain Research* **86**, 440–446.

BALDISSERA, F. & GUSTAFSSON, B. (1974*a*). Afterhyperpolarisation conductance time course in lumbar motoneurones of the cat. *Acta Physiologica Scandinavica* **91**, 512–517.

BALDISSERA, F. & GUSTAFSSON, B. (1974*b*). Firing behaviour of a motoneurone model based on the afterhyperpolarisation conductance time course and algebraical summation. Adaptation and steady state firing. *Acta Physiologica Scandinavica* **92**, 27–47.

BALDISSERA, F., GUSTAFSSON, B. & PARMIGGIANI, F. (1978). Saturating summation of the after hyperpolarisation conductance in spinal motoneurones: a mechanism for 'secondary' range repetitive firing. *Brain Research* **146**, 69–82.

BROWNSTONE, R. M., JORDAN, L. M., KRIELLARS, D. J., NOGA, B. R. & SCHEFCHYK, S. J. (1992). On the regulation of repetitive firing in lumbar motoneurones during fictive locomotion in the cat. *Experimental Brain Research* **90**, 441–455.

CALVIN, W. H. & STEVENS, C. F. (1968). Synaptic noise and other sources of randomness in motoneuron interspike intervals. *Journal of Neurophysiology* **31**, 574–587.

CLAMMAN, P. H. (1969). Statistical analysis of motor unit firing patterns in a human skeletal muscle. *Biophysics Journal* **9**, 1233–1251.

COX, D. R. & ISHAM, V. (1980). *Point Processes.* Chapman and Hall, London.

DAVEY, N. J. & ELLAWAY, P. H. (1988). Control from the brainstem of synchrony of discharge between gamma motoneurones in the cat. *Experimental Brain Research* **72**, 249–263.

DE LUCA, C. J. & FORREST, W. J. (1973). Probability distribution functions of the interpulse intervals of single motor unit action potentials during isometric contractions. In *New Developments in Electromyography and Clinical Neurophysiology*, vol. 1, ed. DESMEDT, J. E., pp. 638–647. Karger, Basel, Switzerland.

ECCLES, J. C., ECCLES, R. M. & LUNDBERG, A. (1958). Action potentials of motoneurones supplying fast and slow muscles. *Journal of Physiology* **142**, 275–291.

ELLAWAY, P. H. (1972). The variability in the discharge of fusimotor neurones in the decerebrated cat. *Experimental Brain Research* **14**, 105–117.

ELLAWAY, P. H. & MURTHY, K. S. K. (1985). The origins and characteristics of cross-correlated activity between γ-motoneurones in the cat. *Quarterly Journal of Experimental Physiology* **70**, 219–232.

ENOKA, R. M., ROBINSON, G. A. & KOSSEV, A. R. (1989). Task and fatigue effects on low-threshold motor units in a human hand muscle. *Journal of Neurophysiology* **62**, 1344–1359.

FARMER, S. F., BREMNER, F. D., HALLIDAY, D. M., ROSENBERG, J. R. & STEPHENS, J. A. (1993). The frequency content of common synaptic inputs to motoneurones studied during voluntary isometric contraction in man. *Journal of Physiology* **470**, 127–155.

FETZ, E. E. & GUSTAFSSON, B. (1983). Relation between shapes of post-synaptic potentials and changes in firing probability of cat motoneurones. *Journal of Physiology* **341**, 387–410.

FREUND, H.-J., DIETZ, V., WITA, C. W. & KAPP, H. (1973). Discharge characteristics of single motor units in normal subjects and patients with supraspinal motor disturbances. In *New Developments in Electromyography and Clinical Neurophysiology*, vol. 3, ed. DESMEDT, J. E., pp. 242–250. Karger, Basel, Switzerland.

GEISLER, C. D. & GOLDBERG, J. M. (1966). A stochastic model of the repetitive activity of neurons. *Biophysical Journal* **6**, 53–69.

GERSTEIN, G. L. & MANDELBROT, B. (1964). Random walk models for the spike activity of a single neuron. *Biophysical Journal* **4**, 41–75.

GOLDBERG, J. M., ADRIAN, H. O. & SMITH, F. D. (1964). Response of neurons of the superior olivary complex of the cat to acoustic stimuli of long duration. *Journal of Neurophysiology* **27**, 517–545.

GRANIT, R. G., KELLERTH, J.-O. & WILLIAMS, T. D. (1964). Intracellular aspects of stimulating motoneurones by muscle stretch. *Journal of Physiology* **174**, 435–452.

GUSTAFSSON, B. & MCCREA, D. (1984). Influence of stretch-evoked synaptic potentials on firing probability of cat spinal motoneurones. *Journal of Physiology* **347**, 431–451.

HILL, A. B. (1961). *Principles of Medical Statistics*, 7th edn. The Lancet, London.

ITO, M. & OSHIMA, T. (1962). Temporal summation of AHP following a motoneuron spike. *Nature* **195**, 910–911.

JACK, J. J. B., MILLER, S., PORTER, R. & REDMAN, S. J. (1971). The time course of minimal excitatory post-synaptic potentials evoked in spinal motoneurones by group Ia afferent fibres. *Journal of Physiology* **215**, 353–380.

JACK, J. J. B, NOBLE, D. & TSIEN, R. W. (1983). *Electric Current Flow in Excitable Cells.* Oxford University Press, Oxford, UK.

KENYON, G. T., PUFF, R. D. & FETZ, E. E. (1992). A general diffusion model for analysing the efficacy of synaptic input to threshold neurons. *Biological Cybernetics* **67**, 133–141.

KERNELL, D. (1968). The repetitive impulse discharge of a simple neurone model compared to that of spinal motoneurones. *Brain Research* **11**, 685–687.

KIRKWOOD, P. A. (1979). On the use and interpretation of cross-correlation measurements in the mammalian central nervous system. *Journal of Neuroscience Methods* **1**, 107–132.

KIRKWOOD, P. A. & SEARS, T. A. (1991). Cross-correlation analyses of motoneuron inputs in a coordinated motor act. In *Neuronal Cooperativity*, ed. KRÜGER, J., pp. 225–248. Springer-Verlag, Berlin.

KRANZ, H. & BAUMGARTNER, G. (1974). Human alpha motoneurone discharge, a statistical analysis. *Brain Research* **67**, 324–329.

LONGUET-HIGGINS, M. S. (1962). The distribution of intervals between zeros of a stationary random function. *Philosophical Transactions of the Royal Society* A **254**, 557–599.

MATTHEWS, P. B. C. (1994). The simple frequency response of human stretch reflexes in which either short- or long-latency components predominate. *Journal of Physiology* **481**, 777–798.

MEUNIER, S., PIERROT-DESEILLIGNY, E. & SIMONETTA-MOREAU, M. (1994). Pattern of heteronymous recurrent inhibition in the human lower limb. *Experimental Brain Research* **102**, 149–159.

MIDRONI, G. & ASHBY, P. (1989). How synaptic noise may affect cross-correlations. *Journal of Neuroscience Methods* **27**, 1–12.

MILES, T. S., TÜRKER, K. S. & LE, H. T. (1989). Ia reflexes and EPSPs in human soleus motoneurones. *Experimental Brain Research* **77**, 628–636.

MOORE, G. P., PERKEL, D. H. & SEGUNDO, J. P. (1966). Statistical analysis and functional interpretation of neuronal spike data. *Annual Review of Physiology* **28**, 493–522.

NORDSTROM, M. A., FUGLEVAND, A. J. & ENOKA, R. M. (1992). Estimating the strength of common input to human motoneurons from the cross-correlogram. *Journal of Physiology* **453**, 547–574.

OLIVIER, E., BAWA, P. & LEMON, R. N. (1995). Excitability of human upper limb motoneurones during rhythmic discharge tested with transcranial magnetic stimulation. *Journal of Physiology* **485**, 257–269.

PERSON, R. S. & KUDINA, L. P. (1972). Discharge frequency and discharge pattern of human motor units during voluntary contraction of muscle. *Electroencephalography and Clinical Neurophysiology* **32**, 471–483.

PIOTRKIEWICZ, M., CHURIKOVA, L. & PERSON, R. (1992). Excitability of single firing human motoneurones to single and repetitive stimulation (experiment and model). *Biological Cybernetics* **66**, 253–259.

POLIAKOV, A. V., MILES, T. S. & NORDSTROM, M. A. (1994). A new approach to the estimation of post-synaptic potentials in human motoneurones. *Journal of Neuroscience Methods* **53**, 143–149.

SCHWINDT, P. C. & CALVIN, W. H. (1972). Membrane-potential trajectories between spikes underlying motoneuron firing rates. *Journal of Neurophysiology* **35**, 311–325.

SCHWINDT, P. C. & CALVIN, W. H. (1973). Equivalence of synaptic and injected current in determining the membrane potential trajectory during motoneuron rhythmic firing. *Brain Research* **59**, 389–394.

SCHWINDT, P. C. & CRILL, W. E. (1982). Factors influencing motoneuron rhythmic firing: results from a voltage-clamp study. *Journal of Neurophysiology* **48**, 875–890.

TOKIZANE, T. & SHIMAZU, H. (1964). *Functional Differentiation of Human Skeletal Muscle.* University of Tokyo Press, Tokyo.

WARREN, J. D., MILES, T. S. & TÜRKER, K. S. (1993). Properties of synaptic noise in tonically active human motoneurons. *Journal of Electromyography and Kinesiology* **2**, 189–202.

Received 20 January 1995; accepted 16 November 1995.